Advancements in thermoelectric generators for enhanced hybrid photovoltaic system performance

Samson Shittu[a]

Guiqiang Li[a, *]

Guiqiang.Li@hull.ac.uk

Yousef Golizadeh Akhlaghi[a]

Xiaoli Ma[a]

Xudong Zhao[a, **]

Xudong.Zhao@hull.ac.uk

Emmanuel Ayodele[b]

[a]School of Engineering and Computer Science, University of Hull, HU6 7RX, UK

[b]Institute of Robotics, Autonomous Systems and Sensing, University of Leeds, LS2 9JT, UK

*Corresponding author.

**Corresponding author.

Abstract

Effective thermal management of photovoltaic cells is essential for improving its conversion efficiency and increasing its life span. Solar cell temperature and efficiency have an inverse relationship therefore, cooling of solar cells is a critical research objective which numerous researchers have paid attention to. Among the widely adopted thermal management techniques is the use of thermoelectric generators to enhance the performance of photovoltaics. Photovoltaic cells can convert the ultra-violent and visible regions of the solar spectrum into electrical energy directly while thermoelectric modules utilize the infrared region to generate electrical energy. Consequently, the combination of photovoltaic and thermoelectric generators would enable the utilization of a wider solar spectrum. In addition, the combination of both systems has the potential to provide enhanced performance due to the compensating effects of both systems. The waste heat produced from the photovoltaic can be used by the thermoelectric generator to produce additional energy thereby increasing the overall power output and efficiency of the hybrid system. However, the integration of both systems is complex because of their opposing characteristics thus, effective coupling of both systems is essential. This review presents the concepts of photovoltaics and thermoelectric energy conversion, research focus areas in the hybrid systems, applications of such systems, discussion of the most recent research accomplishments and recommendations for future research. All the essential elements and research areas in hybrid photovoltaic/thermoelectric generator are discussed in detailed therefore, this review would serve as a valuable reference literature.

Keywords: Hybrid photovoltaic system; Thermoelectric generator; Solar energy; Thermal management; Photovoltaic-thermoelectric

Nomenclature

FF

Fill factor

T

Temperature, K

A

Area, m

C

Concentration ratio

G

Solar irradiance, W/m^2

V_{oc}

Open circuit voltage, V

I_{sc}

Short circuit current, A

P_{in}

Incident power, W

ZT

Figure of merit

Greek symbols

α

Seebeck coefficient, V/K

κ

Thermal conductivity, W/m/K

σ

Electrical conductivity, S/m

η

Efficiency, %

Abbreviations

PV

Photovoltaic

TE

Thermoelectric

PV/TEG

Photovoltaic/thermoelectric generator

TPV/TEG

Thermophotovoltaic/thermoelectric generator

CdTE

Cadmium telluride

CIGS

Copper indium gallium selenide

DSSC

Dye-sensitized solar cell

GaAs

Gallium arsenide

GaSb

Gallium antimonide

$CoSb_3$

Copper antimony

InP

Indium phosphide

Bi_2Te_3

Bismuth telluride

PbTe

Lead telluride

GeTe

Germanium telluride

SnTe

Tin telluride

I-V

Current-Voltage

TEG

Thermoelectric generator

a-Si

Amorphous silicon

c-Si

Crystalline silicon

CZTS

Copper zinc tin sulfide

PCM

Phase change material

SSA

Solar selective absorber

PSC

Perovskite solar cell

EEG

Electroencephalography

AM

Air Mass

LOM

Lock-On mechanism

Subscripts

H

Hot side

C

Cold side

1 Introduction

A consequence of industrialization and the exponential rate at which the world's population is growing is the unprecedented increase in energy demand. Currently, fossil fuel supplies 80% of the world's energy due to the high initial cost of renewable energy systems. However, conventional energy sources like fossil fuel are limited energy sources that cause serious environmental issues which affect the climate and health of the people. Eventually, the global energy demand would outgrow the available energy supply from conventional sources [1,2]. It is therefore imperative to consider renewable energy sources because of their unique advantages such as; inexhaustibility and low pollution. Solar energy is the most abundant renewable energy easily accessible globally. The global energy demand can be met by solar energy due to its vast energy capacity. In fact, the total solar radiation impinged on the energy surface is more than 7500 times the world's total annual primary energy consumption of 450 EJ [3].

Solar photovoltaics is one of the two major solar energy technologies including, solar thermal (Fig. 1). Photovoltaic (PV) cells convert solar radiation into electricity directly however, only about 10–15% of the absorbed solar radiation is converted into electricity while the remainder is either reflected to the ambient environment (heat loss) or absorbed as heat thus, increasing the operating temperature of the PV cell and decreasing its conversion efficiency [4]. Although photovoltaic systems have been commercially available for several years, some of the barriers to their widespread application are: elevated temperature in the PV, limited conversion efficiency and dust accumulation. Consequently, several cooling techniques for PV systems have been proposed and among them, air and liquid based cooling of PV systems are the most mature technologies with practical applications worldwide [5]. Asides these two mature cooling techniques, thermoelectric, heat pipe and nanofluid cooling are viable alternatives which have been investigated. The significance of photovoltaic cooling cannot be overemphasised as it greatly affects the performance of the system. Depending on the cell material used, the PV efficiency decreases by a range of 0.25%–0.5% per degree Celsius [6]. This means that even the slightly decrease in PV

temperature can significantly increase its efficiency therefore, cooling techniques are very essential to PV systems. An effective PV waste heat extraction can enhance the conversion efficiency of the PV and provide additional energy (thermal or electrical) simultaneously.

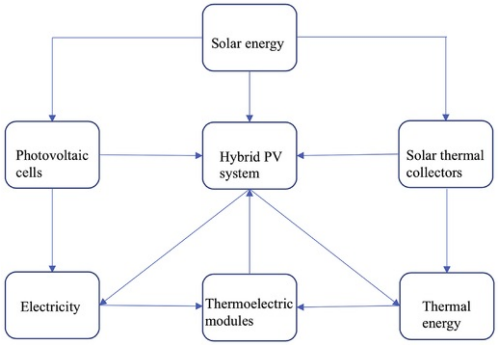

Fig. 1 Solar energy conversion technologies.

alt-text: Fig. 1

Thermoelectric (TE) devices are bi-directional energy converters capable of operating as a generator or cooler. Depending on the operating mode, the TE device can convert electrical energy to thermal energy and vice versa. The advantages of thermoelectric energy converters are; solid-state operation, gas-free emission, maintenance free operation, vast scalability, zero pollution and long-time operational reliability [7,8]. However, low conversion efficiency has limited the widespread application of thermoelectric devices. Geometry optimization and material optimization are the two major solutions being researched for the enhancement of thermoelectric conversion efficiency [9,10]. In addition, the incorporation of TE devices into photovoltaic modules would result in a hybrid device with enhanced overall performance. This is because the two devices (PV and TE) have complimentary characteristics thus, the advantage of the TE can be used to compensate for the disadvantage of the PV. The thermoelectric device can provide dual function of cooling the PV and producing additional energy.

In this study, the most significant advancements made in the efficient thermal management of PV systems using thermoelectric generators are discussed. The aim of the study is to provide a concise review of the role of thermoelectric generators in hybrid photovoltaic performance enhancement. A plethora of literature exists describing the two individual technologies separately (PV and TE) and the field of hybrid Photovoltaic/Thermoelectric (PV/TE) is growing rapidly especially, the integration of thermoelectric generators into Photovoltaic (PV/TEG). Recently, a book on hybrid PV/TEG was written by Narducci et al. [11] which explains the fundamentals of solar harvesting using photovoltaic and thermoelectric generators. This study on the other hand, offers a more condensed review of the main concepts and underling principles of hybrid PV/TEG. The objective of this study is to provide a detailed overview of the current state of art in hybrid photovoltaic-thermoelectric generation. In particular, the main research focus areas in hybrid PV/TEG will be explored thereby providing valuable information on the major issues being tackled in the hybrid system research. Furthermore, the most recent works published on hybrid PV/TEG are analysed in detail and the significance of each study is explored. In addition, this review presents niche applications of hybrid PV/TEG. Finally, recommendations for future research are presented to provide a guide for interested researchers on hybrid PV/TEG. It is envisaged that readers interested in a quick and fundamental understanding of hybrid photovoltaic-thermoelectric generators would find this review very useful while the aforementioned book [11] is recommended for a more in-depth understanding of all issues relating to hybrid PV/TEG. Consequently, this review along with the book will serve as essential and indispensable reference literatures on hybrid PV/TEG.

2 Photovoltaic systems

The photovoltaic effect was first discovered by French physicist, Edmond Becquerel in 1839. However, the first silicon solar cell with a p-n junction was developed in 1954 by a group of researchers led by Chapin D.M at the Bell telephone laboratories [12]. A timeline of the progress on photovoltaic solar energy conversion is shown in Table 1 [13]. Photovoltaic systems can be grouped into three generations and they are [14]:

1) First generation systems: These are fully commercial systems based on crystalline silicon technology. They include monocrystalline and polycrystalline silicon cells.

2) Second generation systems: These are based on the photovoltaic thin film and they include, amorphous silicon, cadmium telluride and indium copper selenide, indium and gallium-diselenide.

3) Third generation systems: These include organic photovoltaic cells that are still in developmental phase and used in niche applications. In addition, Dye-sensitized solar cell and III-V compound (e.g. GaAs, GaSb and InP) are part of this generation of photovoltaic systems.

Table 1 Relevant dates to photovoltaic solar energy conversion [13].

alt-text: Table 1

Scientist	Innovation	Year

Edmond Becquerel	Discovered the photovoltaic effect	1839
William Adams and Richard Day	Noticed the photovoltaic effect in selenium	1876
Max Planck	Predicted the quantum nature of light	1900
Alan Wilson	Proposed the quantum theory of solids	1930
Nevill Mott and Walter Schottky	Developed the theory of solid-state rectifier (diode)	1940
John Bardeen, Walter Brattain and William Shockley	Invented the transistor	1949
Daryl Chapin, Calvin Fuller and Gerald Pearson	Developed a 6% efficient silicon solar cell	1954
D.C Reynold, G. Leies, L.L. Antes and R.E. Marburger	Developed solar cell based on cadmium sulphide	1954
Solar cells were used for the first time on an orbiting satellite Vanguard 1		1958

A photovoltaic cell is made up of p-type and n-type semiconductors that absorb incoming photons and convert them into electron-hole pairs. Basically, electrons are promoted from the valence band to conduction band when the absorbed energy is equal to or greater than the band gap energy. This process generates electron-hole pairs which diffuse and separates at the p-n junction of the semiconductors due to generated electric field. Subsequently, electrons are attracted to the negative side while the holes move to the positive side. Finally, the electrons flow in the external circuit and current is generated as shown in Fig. 2a [15]. Some of the best reported measured efficiency for different solar cell materials are shown in Table 2 [16]. It can be seen that monocrystalline silicon cell still has the best conversion efficiency however, PV material optimization research is still on-going and better efficiency values could be achieved in the future.

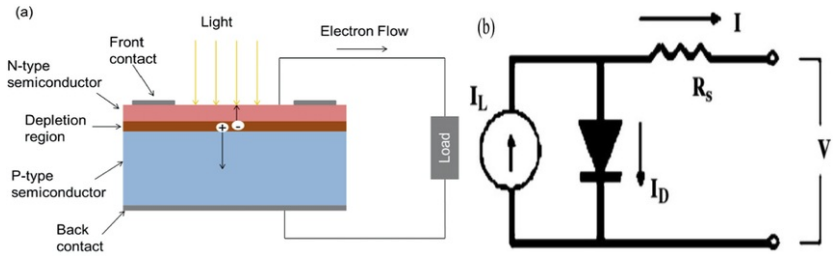

Fig. 2 Photovoltaic cell (a) p-n junction structure [15] and (b) simplified equivalent circuit [13].

alt-text: Fig. 2

Table 2 Confirmed cell efficiency measured under the global Air Mass (AM) 1.5, spectrum (1000 W/m^2) at 25 °C [16].

alt-text: Table 2

Cell type	Efficiency (%)	Description	Reference
Silicon, (monocrystalline cell)	26.7 ± 0.5	Kaneka, n-type rear IBC	[133]
Silicon, (polycrystalline cell)	22.3 ± 0.4′	FhG-ISE, n-type	[134]
III-V, GaAs	28.8 ± 0.9	Alta devices	[135]
III-V, InP	24.2 ± 0.5	NREL	[136]
Thin film, CIGS	22.9 ± 0.5	Solar frontier	[137,138]
Thin film, CdTe	21.0 ± 0.4	First solar, on glass	[139]
Amorphous silicon	10.2 ± 0.3	AIST	[140]
Perovskite	20.9 ± 0.7	KRICT	[141]
Dye sensitized	11.9 ± 0.4	Sharp	[142]

Organic	11.2 ± 0.3	Toshiba	[143]

2.1 Modelling of PV cell

A photovoltaic cell can be modelled as a current source with a parallel diode as shown in Fig. 2b. The diode current can be obtained from the Shockley equation as [13]:

$$I_D = \mathrm{I}_0 \left[\exp\left(\frac{\mathrm{q}\left(\mathrm{V} + \mathrm{I}R_S\right)}{\gamma k T_c} \right) - 1 \right] \quad (1)$$

Reverse saturation current is obtained as,

$$\mathrm{I}_0 = \mathrm{D}\mathrm{T}_{ab}^3 exp \frac{\mathrm{q}\varepsilon_G}{A k \mathrm{T}_{ab}} \quad (2)$$

where D is the diode diffusion factor, T_{ab} is absolute temperature, q is electron charge, ε_G is material band gap energy, k is Boltzmann constant and A is cross sectional area.

Depending on required voltage and current levels, solar cells are connected in series and parallel respectively. The solar cell generator voltage and current can be obtained as,

$$V_g = I_g R_s \frac{N_s}{N_p} \ln\left(1 + \frac{N_p \mathrm{I}_{ph} - I_g}{N_p \mathrm{I}_0}\right) \quad (3)$$

where R_s is the series resistance, N_s is number of cells in series, N_p is number of cells in parallel and I_{ph} is the cell photocurrent proportional to solar irradiance.

$$I_g = \mathrm{I}_{ph} - \mathrm{I}_0 \, exp\left(\frac{\mathrm{q}V_g}{kT} - 1\right) \quad (4)$$

where T is the cell temperature.

The PV cell short circuit current (I_{sc}) can be obtained by setting $V_g = 0$ and $I_{sc} = I_{ph}$. This value varies with cell irradiance and the PV cell open circuit voltage (V_{oc}) can be obtained by setting $I_g = 0$ thus,

$$\mathrm{V}_{oc} = \frac{kT}{\mathrm{q}} \ln\left[\frac{\mathrm{I}_{ph}}{\mathrm{I}_0}\right] \quad (5)$$

The maximum output power of the PV is expressed as,

$$\frac{\mathrm{d}\left(V_g \times I_g\right)}{dt} = 0 \quad (6)$$

$$\mathrm{V}_{mp} = \mathrm{V}_{oc} - \frac{kT}{\mathrm{q}} \ln\left[\frac{\mathrm{V}_{mp}}{kt/\mathrm{q}} + 1\right] \quad (7)$$

The fill factor (FF) can be expressed as,

$$FF = \frac{\mathrm{V}_{mp} \times \mathrm{I}_{mp}}{\mathrm{V}_{oc} \times \mathrm{I}_{sc}} \quad (8)$$

The efficiency of the PV can be expressed as,

$$\eta_{pv} = \frac{FF \times \mathrm{V}_{oc} \times \mathrm{I}_{sc}}{\mathrm{P}_{in}} \quad (9)$$

where P_{in} is the incident power on the PV cell.

2.2 Influence of temperature on photovoltaic cells

Majority of the research on PV system has been on efficiency enhancement by application of effective thermal management techniques. The conversion efficiency of the PV is largely dependent on the solar cell temperature therefore, cooling of the PV is of utmost importance. It is obvious from Fig. 3 that the solar cell temperature affects the cell efficiency, open circuit voltage and short circuit current [17]. In addition, Fig. 4 shows the influence of cell temperature on the current-voltage (I-V) characteristics of the PV cell [18].

Generally, the PV performs better at lower cell temperature values. The temperature dependence of PV's efficiency is often characterized by a property known as Temperature coefficient. It is used in quantifying the temperature sensitivities of the PV cell performance. To compare different PV cells, the temperature coefficient are usually given at a normalized value of 25 °C or 298.15 K [19].

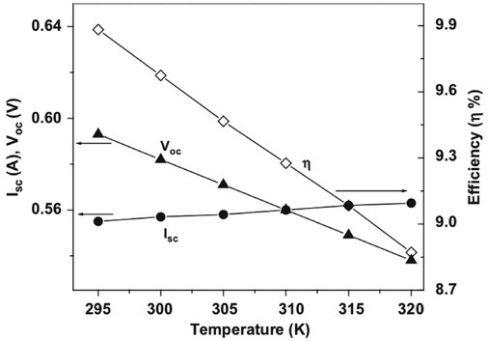

Fig. 3 Effect of cell temperature on efficiency, open circuit voltage and short circuit current of a monocrystalline silicon cell [17].

alt-text: Fig. 3

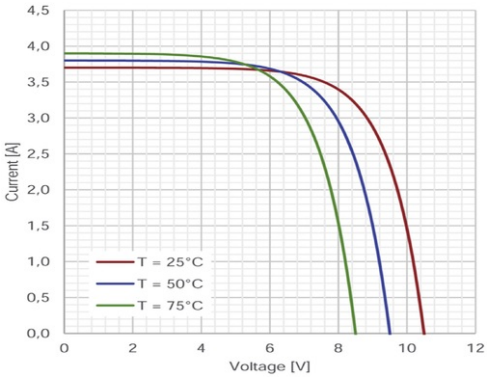

Fig. 4 Influence of temperature on the I-V characteristics of a photovoltaic cell [18].

alt-text: Fig. 4

The PV electrical efficiency can be increased by removing the accumulated heat from the concealed PV surface and using this heat appropriately [20]. Different technologies such as Photovoltaic/Thermal (PV/T) and Photovoltaic/Thermoelectric Generator (PV/TEG) have been developed for this purpose. However, the PV/TEG can only fulfil this purpose if the TEG is in physical contact with the PV (i.e. direct coupling method). Nevertheless, the TEG will have to operate at a temperature higher than the ambient temperature to produce some electrical power and it most likely will heat up the solar cell if not properly cooled. If the TEG is not in physical contact with the PV (i.e. spectrum splitting method), it cannot cool down the PV cell.

3 Thermoelectric devices

Thermoelectric devices can generate electrical power from thermal energy via the Seebeck effect as shown in Fig. 5a. When a temperature gradient (ΔT) is applied to a thermoelectric couple made up of n-type and p-type semiconductor materials, the mobile charge carriers located at the hot end (heat source) diffuse to the cold end (heat sink) thus, an electrostatic potential (ΔV) is produced. This process is known as the Seebeck effect which was discovered in 1821 by Thomas Seebeck. The Seebeck coefficient is an intrinsic thermoelectric material property which is expressed as,

$$\alpha = \Delta V / \Delta T \quad \textbf{(10)}$$

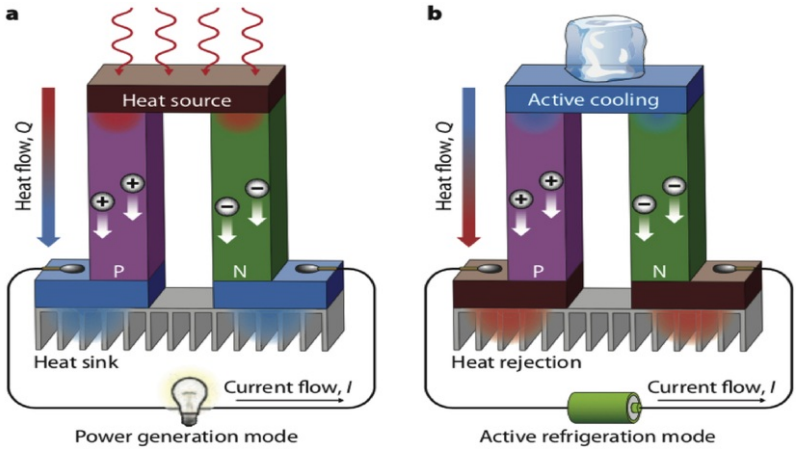

Fig. 5 Schematic of a thermoelectric (a) generator and (b) cooler [21].

alt-text: Fig. 5

On the contrary, the application of a current on a thermoelectric couple causes the charge carriers to attempt to return to the electron equilibrium that existed before the current was applied by absorbing or releasing energy at the interface of two dissimilar materials. This process is known as the Peltier effect which was discovered in 1834 by Jean-Charles Peltier and it is shown in Fig. 5b [21].

The Thomson effect which was discovered in 1852 by William Thomson is the last of the thermoelectric effects and it is related to the rate of reversible heat q generation. The reversible heat results from current passing through a portion of a single conductor along which there is a temperature difference. Although Thomson effect is not of primary importance in thermoelectric devices, it is still essential for detailed calculations as it influences the device performance [22].

3.1 Thermoelectric materials

The quality of thermoelectric materials used for generating electric power via the Seebeck effect or cooling (refrigeration) via the Peltier effect is mainly determined by three intrinsic material properties including, electrical conductivity, seebeck coefficient and thermal conductivity. Materials with high electrical conductivity are favourable because electrical current is passed in both the power generation and cooling mode. In addition, a large seebeck coefficient is essential because a large generated voltage per unit temperature gradient is desired. Lastly, a low thermal conductivity is essential for TE materials because temperature difference must be maintained across the material [23]. A dimensionless parameter known as thermoelectric figure of merit (ZT) is usually used to obtain the thermoelectric efficiency and it is expressed as [24],

$$ZT = \frac{\alpha^2 \sigma}{\kappa} \mathrm{T} \tag{11}$$

where α is the Seebeck coefficient, σ is the electrical conductivity, κ is the thermal conductivity and T is the absolute temperature.

Generally, materials with high ZT are preferable however, optimizing all the intrinsic material properties that influence the ZT together at once is very difficult because they are interdependent and reciprocal. This challenge caused the maximum ZT of any thermoelectric material to remain at $ZT \approx 1$ for almost fifty years [23]. However, due to the extensive material research been undertaken, there has been reported progress in overcoming the limitations and increasing the thermoelectric figure of merit greatly. Two approaches have been investigated including, modifying the material microstructure to increase photon scattering thus, decreasing the thermal conductivity. Materials such as skutterudites, clathrates and chalcogenides have been optimized using this approach. The other approach is to reduce the material dimensionality in order for quantum size-effects to alter the ration between the electrical and thermal conductivity [25]. In addition, efforts have been made to increase the ZT of materials by adding other semiconductor or nanostructure materials. It was found that the figure of merit for nanostructure materials is 3 at 300 °C and it varies from 0.4 to 1.1 at low temperature difference value like 27 °C [26,27]. This is a much higher value than the typical ZT value (0.8) of commercial materials like n-type Bi_2Te_3 and p-type Sb_2Te_3 at temperatures below 150 °C [24]. Super-lattice structure, plasma treatment and material segmentation are the other methods used in developing thermoelectric materials with high efficiency [28].

Classifying thermoelectric materials based on operating temperature range, Bismuth telluride (Bi_2Te_3) is used for low temperature (<500 K) power generation. Materials based on group-IV tellurides such as PbTe, GeTe and SnTe are used for mid-temperature (500–900 K) power generation. Lastly, silicon-germanium alloys are used for high temperature (>900 K) power generation [29]. For thermoelectric devices to gain wider application, materials with high ZT and low price must be developed, and this is an achievable future goal due to the extensive research being carried out in this area.

3.2 Modelling of thermoelectric generator and cooler

The efficiency of a thermoelectric generator is expressed as [22],

$$\eta = \frac{Energy\ \ supplied\ \ to\ \ the\ \ load}{Heat\ \ energy\ \ abosrbed\ \ at\ \ the\ \ hot\ \ junction} \tag{12}$$

Assuming constant thermoelectric material properties and negligible contact resistances, the efficiency can be expressed as,

$$\eta_{teg} = \frac{\mathrm{I}^2\mathrm{R}}{\alpha I T_H = \kappa\left(T_H - T_C\right) - \frac{1}{2}\mathrm{I}^2\mathrm{R}} \tag{13}$$

where I is current, R is series resistance, T_H is hot side temperature and T_C is cold side temperature.

The maximum conversion efficiency is given as,

$$\eta_{max} = \eta_c \frac{\sqrt{1+ZT}-1}{\sqrt{1+ZT}+\frac{T_C}{T_H}} \tag{14}$$

where η_c is the Carnot efficiency and it is expressed as,

$$\eta_c = \frac{T_H - T_C}{T_H} \tag{15}$$

The energy efficiency of the thermoelectric cooler is measured in terms of its coefficient of performance (COP) and it is expressed as [22],

$$COP = \frac{Heat\ \ absorbed}{Electrical\ \ power\ \ input} = \frac{\alpha I T_C - \frac{1}{2}\mathrm{I}^2\mathrm{R} - \kappa\left(T_H - T_C\right)}{\alpha I\left(T_H - T_C\right) + \mathrm{I}^2\mathrm{R}} \tag{16}$$

The current $\bar{\mathrm{I}}$ for maximum cooling power is expressed as,

$$\bar{\mathrm{I}} = \frac{\alpha T_C}{\mathrm{R}} \tag{17}$$

The maximum coefficient of performance is given as,

$$COP_{max} = \frac{T_C\left[(1+ZT)^{\frac{1}{2}} - \frac{T_H}{T_C}\right]}{\left(T_H - T_C\right)\left[(1+ZT)^{\frac{1}{2}} + 1\right]} \tag{18}$$

As in the case of the thermoelectric generator, the figure of merit (ZT) also determines the maximum coefficient of performance that can be achieved.

3.3 Applications of thermoelectric generator and cooler

Thermoelectric generators have a wide range of applications such as in waste heat recovery for automobiles [30–33], wearable sensors [34–37], micropower generation [38], wireless sensor network [39], space power [40] and buildings [7]. Thermoelectric coolers are used in cooling electronic devices [41], refrigerators and air conditioners [29] and for specific applications in military, aerospace, instrument, biology, medicine and industrial products [41]. Detailed explanation of the application of the thermoelectric generator and cooler in the aforementioned sectors can be found in the referenced literatures. For the sake of this review, more focus is placed on the application of hybrid PV/TEG in the later sections.

4 Hybrid photovoltaic/thermoelectric generator (PV/TEG)

Integrating thermoelectric devices into photovoltaic systems can enable the efficient thermal management of PV thus, enhancing its overall performance. When thermoelectric generators are combined with PV, depending on the integration method of the PV/TEG, the TEG can utilize the waste heat from the PV to generate some electrical energy if it is properly cooled and there is sufficient temperature difference across it. In addition, the overall hybrid system performance could potentially be enhanced by the integration of thermoelectric generators into PV if the system is properly designed although the is a possibility of reduced performance due to the complex relationship between PV and TEG.

Similarly, thermoelectric coolers can be used to remove the waste heat from the PV and enhance the overall hybrid system performance. Research on hybrid PV/TEG dates back to 1988 when Moore and Peterson [42] designed a hybrid system with the intention

of using the PV to supply power during high solar irradiance periods while using the TEG to provide power and heat during periods of low solar irradiance. The authors examined two existing sites in Northern Canada, and they concluded that at locations where delivered fuel costs was significant and conventional PV wasn't available, the hybrid PV/TEG could provide unmatched reliability and economics.

4.1 Modelling of hybrid PV/TEG

Generally, the overall efficiency of the hybrid PV/TEG is a sum of the individual efficiencies of the PV (η_{pv}) and TEG (η_{teg}) and it can be expressed as [11]:

$$\eta_{pv/teg} = \eta_{pv} + \eta_{teg} = \frac{\mathrm{P}_{pv}}{\mathrm{P}_{in}\mathrm{A}_{pv}} + \frac{\mathrm{P}_{teg}}{\mathrm{P}_{in}\mathrm{A}_{pv}} \tag{19}$$

where P_{pv} is the power output of the solar cell, P_{teg} is the TEG power output, A_{pv} is the solar cell area and P_{in} is the input solar power.

The above Eq. (19) is applicable for a simplified design of a hybrid PV/TEG where the PV and TEG are thermally coupled but electrically separated.

Considering the efficiencies of all the main components of the PV/TEG including, optical collector, opto-thermal converter, thermal collector, thermoelectric convert and thermal dissipater, the hybrid system efficiency can also be defined as [11]:

$$\eta_{pv/teg} = \eta_{pv} + \eta_{teg} = \eta_{pv} + \eta_{opt}\eta_{ot}\eta_{teg}\eta_{diss} \tag{20}$$

where η_{opt} is the optical collector efficiency, η_{ot} is the opto-thermal efficiency and η_{diss} is the thermal dissipater efficiency.

The optical collector efficiency is given as:

$$\eta_{opt} = \frac{\mathrm{CP}_{in}\mathrm{A}_{opt}\tau_{opt}}{\mathrm{CP}_{in}\mathrm{A}_{opt}} = \tau_{opt} \tag{21}$$

where C is the optical concentration, A_{opt} is the optical collector aperture area and τ_{opt} is either the optical collector transmittance or reflectivity, depending on the optical component used (i.e. lens or mirror). Normally, τ_{opt} is expected to be ≥ 0.9 therefore, the optical collector can be assumed to not absorb power thus, it does not heat up. Consequently, η_{opt} can be considered as temperature independent.

The thermal dissipater efficiency is given as:

$$\eta_{diss} = 1 - \frac{\mathrm{P}_{diss}}{\mathrm{P}_{steg}^{out}} \tag{22}$$

where P_{diss} is the electrical power needed to circulate the cooling fluid and P_{steg}^{out} is the electrical power output of the solar TEG. When passive dissipation is considered (i.e. $\mathrm{P}_{diss} = 0$), $\eta_{diss} = 1$ while when active dissipation is considered, the details of the heat dissipater geometry has to be considered.

The opto-thermal efficiency of the hybrid system is given as:

$$\eta_{ot} = \alpha_{otconv}\tau_{enc}\tau_{hm}\left[1 - \left(\eta_{pv} + \mathrm{R}_{pv} + \mathrm{T}_{pv}\right)\right] - \frac{\sigma \mathrm{A}_{abs}\left[\varepsilon'_{pv}\left(T_h^4 - T_a^4\right) + \varepsilon_{thcol'}\left(T_h^4 - T_c^4\right)\right]}{\mathrm{CP}_{in}\tau_{opt}\mathrm{A}_{opt}} \tag{23}$$

where the assumption is that the TEG hot side temperature is equal to the solar cell temperature (i.e. $T_h = T_{pv}$). This assumption is only valid for the case of direct coupling method. For the spectrum splitting method, it is assumed that the solar cell temperature is equal to the temperature of the encapsulation (i.e. $T_{pv} = T_{enc}$). Therefore, it is important to understand that the opto-thermal efficiency is different for the spectrum splitting and direct coupling methods. In fact, the opto-thermal efficiency is smaller for the case of spectrum splitting method compared to direct coupling method [43]. The reason for this behaviour is that in solar cells, the majority of the thermal losses is actually in the range of energies higher than the energy gap (not in the infrared region), for which the spectrum splitting method cannot act as a recovery strategy [44]. Furthermore, α_{otconv} is opto-thermal convert absorbance, τ_{enc} is transmittance of the possible encapsulation, τ_{hm} is the heat mirror transmittance, ε'_{pv} encompasses the heat reflection properties of the heat mirror, A_{abs} is opto-thermal converter area, T_a is ambient temperature and R_{pv} is the reflected fraction of solar power by the solar cell.

The resultant emittance of the TEG parallel surfaces can be defined as [45]:

$$\varepsilon_{thcol'} = \frac{1}{\frac{1}{\varepsilon_{thcol}} + \frac{1}{\varepsilon_c} - 1} \tag{24}$$

where ε_{thcol} is the thermal collector emittance and ε_c is emittance.

When heat mirrors are used, the solar cell emittance ε_{pv} is replace by an effective emissivity which is defined as [11]:

$$\varepsilon'_{pv} = \varepsilon_{pv}\left(1 - \eta^{r}_{hm}\right) \tag{25}$$

where η^{r}_{hm} is the back-reflecting efficiency for the heat coming from the solar cell and it is defined as:

$$\eta^{r}_{hm} = \left[\left(\frac{\int \mathrm{R}_{hm}(\lambda)\, d\lambda}{\int d\lambda}\right)_{ir}\right] \tag{26}$$

where $R_{hm(\lambda)}$ is the reflectance of the heat mirror and the subscript 'ir' represents the evaluation of the integral over a range of wavelengths from 2500 to 30,000 nm.

From Eq. (20), the efficiencies of some of the hybrid system components (i.e. η_{pv}, η_{teg} and η_{ot}) are temperature dependent and their variation with temperature is shown in Fig. 6 [11]. It is obvious from Fig. 6 that the PV and TEG have an opposite tendency with temperature variation. As expected, the efficiency of the PV (η_{pv}) decreases as the temperature increases while the efficiency of the TEG (η_{teg}) increases as the temperature increases. This is because the PV is more efficient at lower temperature values while the TEG operates better when a large temperature difference is present across its hot and cold side terminals. This opposing trend show the complex relationship between a PV and a TEG. In addition, all the heat produced in the PV cannot be converted by the TEG because there is usually heat loss to the ambient from the PV due to convection and radiation. Furthermore, when the surface area of the TEG is smaller than that of the PV it is attached to directly, a large quantity of the heat produced by the PV may be dissipated directly to the ambient without passing through the TEG.

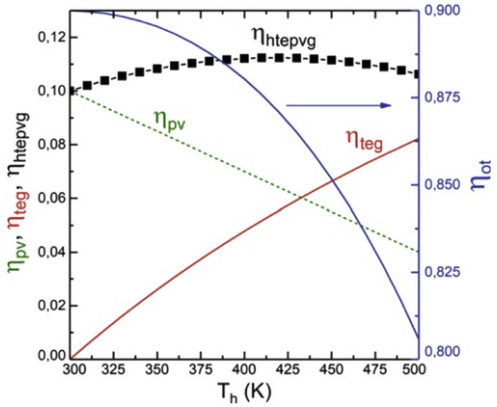

Fig. 6 Variation of hybrid system and individual components efficiency with temperature [11].

alt-text: Fig. 6

Asides the thermal coupling of hybrid PV/TEG which Eq. (19) describes, the PV and TEG can also be electrically connected to form a hybrid system. In the thermal coupled system, the PV and TEG generate electrical power independently while in the electrically coupled system, the TEG can be connected in series or parallel with the PV as shown in Fig. 7 [11]. The overall efficiency of the hybrid system when it is electrically coupled is different from that of the thermal coupling therefore, it is given as [11]:

$$\eta_{pv/teg} = \eta_{pv} + \eta_{steg} - \left(1 - \eta_{el}\right) = \frac{\mathrm{P}_{pv} + \mathrm{P}_{steg} - \mathrm{P}_{el-loss}}{\mathrm{P}_{in}\mathrm{A}_{pv}} \tag{27}$$

where η_{steg} is the solar TEG efficiency, η_{el} is the electrical hybridization efficiency and $P_{el-loss}$ is the electrical power loss.

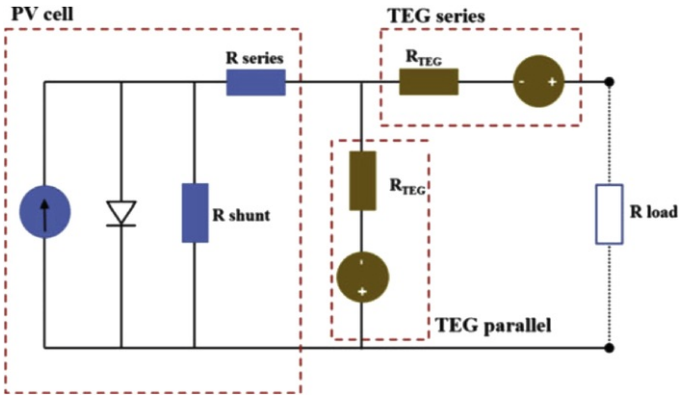

Fig. 7 Equivalent circuit of an electrically connected PV/TEG [11].

alt-text: Fig. 7

4.2 Hybrid system integration methods

The combination of photovoltaic and thermoelectric allows for the wider use of the solar spectrum. This is because PV converts the ultra-violent and visible regions (200–800 nm) of the solar spectrum into electricity while TEG converts the infrared region (800–3000 nm) into electricity [46]. The two main PV/TEG integration methods are the spectrum splitting and direct coupling integration. The difference is the presence or absence of a reflective component (e.g. spectrum-splitter or prism). Determining the best integration method for the hybrid system by comparing the two integration methods (spectrum splitting and direct coupling) is not straightforward. This is because, when conversion efficiency is used as the only comparison parameter, the direct coupling hybrid system can perform better than the spectrum splitting hybrid system [43]. However, the spectrum splitting hybrid system has an advantage over the direct coupling hybrid system because it requires a smaller quantity of active thermoelectric material per unit area due to the smaller hybrid system fill factors at maximum efficiency. In addition, the spectrum splitting system requires a smaller area which must be covered by cooling devices thus, the costs of the spectrum splitting system should be lower than that of the direct coupling system [47]. Nevertheless, the larger size of the system along with the additional cost of the splitting device might result in a balance between the pros and cons of the spectrum splitting and direct coupling integration methods [43]. Consequently, the final decision on the best integration method for the hybrid system can only be reached upon completion of a detailed comparison between the pros and cons (including a cost evaluation) of the two integration methods [47]. Integrating thermoelectric generators into solar panels could provide an additional energy of 2–10% depending on the thermoelectric material, connection and configuration [48]. Therefore, research on PV/TEG is increasing expeditiously due to its huge potential to provide enhanced performance compared to stand alone PV or TEG systems.

4.2.1 Spectrum splitting method

Basically, in the spectrum splitting system, the solar radiation is reflected by a splitter at a specific wavelength (cut-off wavelength) and this separates the radiation used by the PV and TEG for energy conversion as shown in Fig. 8. The PV and TEG are usually placed perpendicularly when the spectrum splitting integration method is used and the radiation that is longer than the cut-off wavelength is reflected by the TEG while those shorter than the cut-off wavelength transmit through the spectrum splitter and are absorbed by the PV [15]. It is important to note that when this integration method is used, the PV and TEG work independently on converting solar energy into electricity thus, the TEG doesn't cool down the PV or use the PV's waste heat for energy conversion.

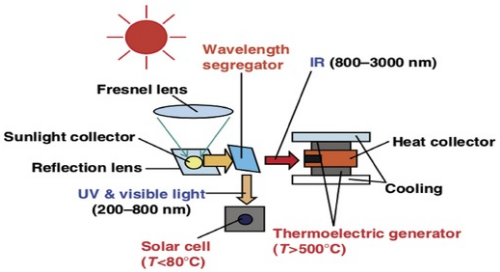

Fig. 8 Schematic of spectrum splitting PV/TEG integration [46].

alt-text: Fig. 8

Kraemer et al. [49] presented a general optimization methodology for a hybrid PV/TEG system using the spectrum splitting method. Three different PV types were studied experimentally, and it was found that the amorphous silicon cell provided the best hybrid system efficiency of

13.26% when a TEG with efficiency of 8% was used. In addition, the authors argued that the hybrid system maximum efficiency was highly dependent on both the solar cell spectral efficiency and the solar TEG efficiency. Furthermore, the authors argued that the short wavelength region directed to the solar TEG is usually only a small portion of the total solar spectrum thus, it could be neglected. Regardless, it is worth noting that the authors used an assumed efficiency value for the TEG which may not be practical.

A comprehensive study of a spectrum splitting concentrated PV/TEG system was performed by Ju et al. [50]. The influence of cut-off wavelength, concentration ratio and heat transfer coefficient on the performance of the hybrid system were studied and optimization of the hybrid system was performed. The investigated system consisted of a solar concentrator, PV cell, TEG, spectral beam splitter and water-cooling system. Two significant ways to improve the efficiency of hybrid systems were proposed by the authors including, increasing the concentration ratio and improving the cooling system performance. In addition, they found that the TEG contributed about 10% of the total hybrid system power and the optimized hybrid system efficiency was about 27.49%. Furthermore, it was found that the concentration ratio has an almost linear relationship with the cooling system heat transfer coefficient. Also, the authors concluded that the solar cell band gap essentially determined the optimized cut-off wavelength of the hybrid system. Finally, a comparison of the hybrid system with the conventional PV system was made and it was found that the hybrid system is better suited for high concentration conditions due to its enhanced performance. Although the results from this research are significant, an experimental validation of the simulation results wasn't performed.

Furthermore, the optimum design for a concentrated spectrum splitting PV/TEG was proposed by Yin et al. [51] to optimize the distribution of solar energy in a spectrum splitting CPV/TEG without compromising the optimum design state of the individual systems. The optimum hybrid system operating temperature and cut off wavelength were presented. In addition, the effect of thermoelectric figure of merit and cooling system convective heat transfer coefficient were discussed. The authors argued that the thermoelectric structure factor influences the optimum temperature distribution in the TEG. It was also found that the spectral splitter optimum cut-off wavelength and thermoelectric figure of merit have an inverse relationship. Yang et al. [52] studied the performance of a spectrum splitting PV/TEG system using numerical simulation. Optimization of the hybrid system cut-off energy, cell voltage and TEG dimensionless current was done and the influence of the area ratio of the collector to PV on the hybrid system performance was studied. It was found that the efficiency of the hybrid system increased by 2.67% and 2.19% compared to that of the PV only system at concentration factors of 30 and 100 respectively.

Bjørk et al. [53] studied the maximum theoretical performance of a PV/TEG system without concentration. The authors used an analytical model to study the performance of the system and found that the hybrid system using spectrum splitting could achieve a maximum efficiency increase of 1.8% point compared to the PV only system. Furthermore, Liang et al. [54] performed an experimental and numerical investigation on the performance of a spectrum splitting concentrated hybrid PV/TEG system. To optimize the performance of the thermoelectric generator in converting the higher wavelength (infrared) into electricity, a cascaded thermoelectric generator configuration was utilized by the authors. The system consisted of two individual TEG stages in which middle temperature thermoelectric material ($CoSb_3$) and low temperature thermoelectric material (Bi_2Te_3) were used for the two stages. The numerical study involved the optimization of the thermoelectric geometry and optical concentration ratio. Results showed that the direct normal irradiation (DNI), optical concentration ratio and height ratio of the two TEG stages could significantly affect the performance of the hybrid PV/TEG system. In addition, results showed that the TEG subsystem, PV subsystem and overall hybrid system efficiencies were 8%, 44% and 35% respectively when DNI = 1000 W/m^2, optical concentration ratio was 1000 and optimized height ratio of the two stage TEG was 0.6. The performance data for some of the spectrum splitting PV/TEG systems reviewed can be found in Table 4.

Table 3 Power output and efficiency enhancement of hybrid system using different cooling systems [103].

alt-text: Table 3

	Natural cooling	Forced cooling	Water cooling	SiO_2/water nanofluid cooling	Fe_3O_4/water nanofluid cooling
Total power increase (%)	Base	4.885	5.776	8.26	6.284
Total efficiency increase (%)	Base	1.865	3.051	3.355	3.131

Table 4 Summary of some selected spectrum splitting PV/TEG systems reviewed.

alt-text: Table 4

Reference	Material		Study type	Efficiency		Remarks
	PV	TE		PV/TEG	PV	
Kraemer et al. [49]	Monocrystalline silicon	N/A	Simulation	11.45%	9.09%	TEG efficiency of 8% corresponding to figure of merit (ZT = 1.7) was used.
	Amorphous silicon	N/A	Simulation	13.26%	9.40%	
	Polymer thin film	N/A	Simulation	8.32%	3.41%	
Ju et al. [50]	GaAs	Skutterudite $CoSb_3$	Simulation	27.49%	N/A	Figure of merit (ZT = 1.4) at 800 K, heat transfer coefficient of 4500 W/m^2/K were used, and the optimized results were given.
Mizoshiri et al. [144]	Amorphous silicon	Thin- film Bismuth	Experiment	N/A	N/A	Open circuit voltage of hybrid system increased by 1.3% compared to PV only system.

Li et al. [95]	N/A	N/A	Simulation	31–34%	N/A	Figure of merit (ZT = 1) was used and 30% power output enhancement was obtained.
Elsarrag et al. [145]	Monocrystalline silicon	Bismuth telluride	Experiment and simulation	N/A	N/A	Hybrid system performed better than PV only system.
Skjølstrup et al. [146]	Amorphous silicon	N/A	Simulation	19.1%	15.8%	Beam splitter layer was 114 and TE efficiency was 8%.
	Microcrystalline silicon	N/A	Simulation	19.8%	17.5%	Beam splitter layer was 128 and TE efficiency was 8%.
Sibin et al. [147]	N/A	N/A	Experiment	N/A	N/A	ITO/Ag/ITO spectral beam splitter coating was developed, and it had a high visible transmittance of 88%.
Yin et al. [51]	GaAs	N/A	Simulation	30%	N/A	Figure of merit was 1 and cut-off wavelength was equal to maximum wavelength of PV.
Yang et al. [52]	Silicon	N/A	Simulation	40.2%	39.32%	Concentration factor was 100.
Bjørk et al. [53]	N/A	N/A	Simulation	1.8% points increase	N/A	Maximum hybrid system efficiency without concentration was studied.
Djafar et al. [148]	N/A	Bismuth telluride	Experiment	N/A	N/A	Long wavelengths of around 800 nm were emitted by the halogen lamps for the TEG.
Shou et al. [149]	Crystalline silicon	N/A	Simulation	3.24% increase	N/A	Hybrid system had a filter at 150 suns.

4.2.2 Direct coupling method

In the direct coupling system, no splitter is used thus, the PV and TEG are directly coupled and placed in a parallel arrangement. The PV is placed directly above the TEG and a heat sink is attached to the bottom of the TEG just as in the case of the spectrum splitting as shown in Fig. 9. The reason for placing the PV above the TEG is because the PV absorbs the shorter wavelengths while the TEG absorbs the longer wavelength [15]. In addition, when the direct coupling method is used, the unabsorbed solar radiation from the PV transmit through the PV to the TEG below and this serves as the input heat flux for the TEG to generate some electrical power.

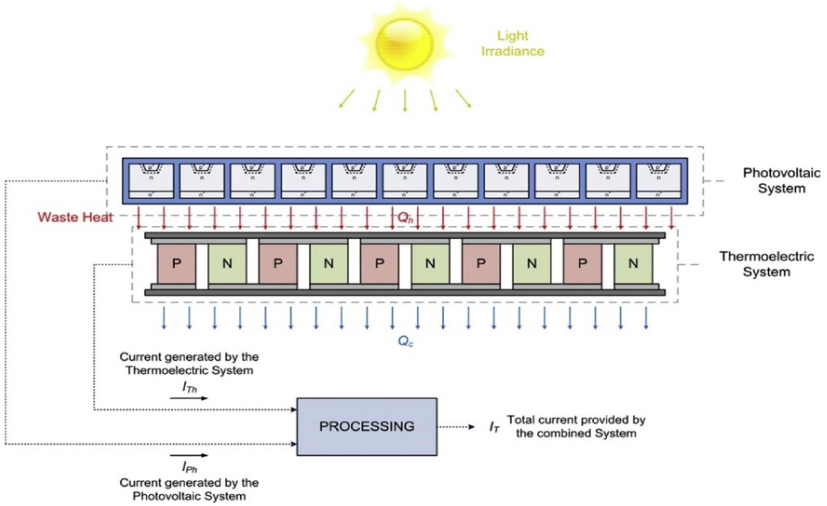

Fig. 9 Schematic of direct coupling PV/TEG integration [18].

alt-text: Fig. 9

Van Sark [55] proposed an effective thermal management technique for photovoltaic cells by integrating thermoelectric modules into the PV using the direct coupling method to form a hybrid PV/TEG system with enhanced electrical performance. Two case studies were presented for Malaga, Spain and Utrecht, Netherlands. In addition, the annual energy yield was calculated using the weather data from the two locations and the authors also presented efficiency enhancement predictions based on future thermoelectric materials to be developed. A series of thermoelectric modules were attached to the back side of the PV while a heat sink was used to maintain a temperature difference of about 50–60 °C. The variation of the hybrid system generated power with solar irradiance for different figure of merit values and PV conditions is shown in Fig. 10a. As expected,

the highest generated power was from the hybrid system with the highest figure of merit value (Z = 0.01/K). In addition, Fig. 10b shows the generated energy from the hybrid system for 10 days in August for Malaga, Spain. The advantage of the PV/TEG over the individual PV and TE systems can be seen clearly from this figure for all the days considered. Using typical figure of merit value of 0.004/K at 300 K, the authors observed an efficiency increase of 23% for the roof integrated PV-TEG. The results obtained also showed that by using the annual irradiance and temperature profiles of Malaga and Utrecht, the annual energy of these cities could increase by about 14.7% and 11% respectively. However, when an assumed high figure of merit value (Z = 0.01/K) from future developments in TE material was used, efficiency increase of about 50% and annual energy increase of 24.9% were predicted by the authors. Notwithstanding, this research ignored radiation loss on the front cover and the idealized model developed, overestimated the results by about 10% for practical PV/TEG systems.

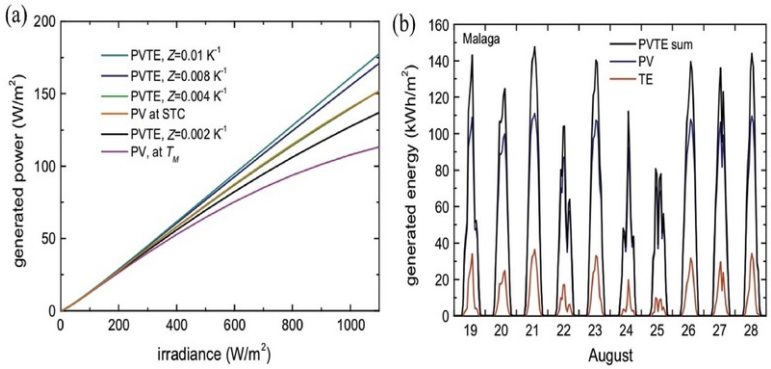

Fig. 10 Hybrid PV/TEG system (a) generated power for four figure of merit Z values and (b) total energy for 10-day period in August for Malaga, Spain [55].

alt-text: Fig. 10

Yin et al. [56,57] performed a couple of detailed investigation on the optimum design of hybrid PV/TEG system using direct coupling method. The actual performance of a PV/TEG system throughout a single day was studied to see the influence of solar radiation variation with time on the hybrid system performance [56]. The changes in the hybrid system temperature and power efficiency within a day were presented and the influence of PV temperature coefficient, thermoelectric figure of merit, water cooling mass and velocity were discussed. The results obtained showed that the hybrid system performed better than the PV only system within a one-day period and a high efficiency of 16.7% was achieved by the hybrid system [56]. Furthermore, an optimum design method and selection principle for a concentrated direct coupling PV/TEG system was presented in Ref. [57]. Firstly, the temperature distribution corresponding to the optimum hybrid system efficiency was calculated and then the optimum TEG thermal resistance corresponding to the optimum hybrid system temperature distribution was calculated. Lastly, the optimum TEG structure was determined after the two previous steps and the influence of thermoelectric figure of merit and cooling system convective heat transfer coefficient on the hybrid system performance were investigated. It was found that the minimum TEG figure of merit value can be used to perform a feasibility study for the CPV/TEG and select the coupling devices. The authors also found that the optimum temperature and thermoelectric thermal resistance both have an inverse relationship with the PV temperature coefficient. Recently, Li et al. [58] performed a comparative study of the optimum geometry for thermoelectric elements in a direct coupling photovoltaic-thermoelectric and solar thermoelectric system. The optimum geometry for enhanced PV-TE and STEG performance was investigated using finite element method. Two photovoltaic cells and different thermoelectric leg geometries were studied and compared with a solar thermoelectric generator. The effects of environmental conditions like solar radiation and concentration ratio were also studied and the results obtained showed that the optimum thermoelectric element geometry in a hybrid PV/TEG system was dependent on the characteristics of the solar cell used and this optimum geometry is different from that of the solar thermoelectric generator under similar conditions. The performance data for some of the directly coupling PV/TEG systems reviewed can be found in Table 5.

Table 5 Summary of some selected direct coupling PV/TEG systems reviewed.

alt-text: Table 5

Reference	Material		Study type	Efficiency		Remarks
	PV	TE		PV/TEG	PV	
Guo et al. [104]	Dye-sensitized solar cell (DSSC)	N/A	Experiment	10% increase	N/A	Hybrid efficiency was compared with a single DSSC.
Wang et al. [105]	Dye-sensitized solar cell	N/A	Experiment	13.8%	9.26%	Solar selective absorber was used.
Sark [55]	Polycrystalline silicon	Bismuth telluride (Bi_2Te_3)	Simulation	13.98%	10.78%	Typical figure of merit value of 1.2 and coefficient c = 0.058 were used.
Daud et al. [150]	Polycrystalline silicon	Bismuth telluride	Experiment	9.064%	5.970%	Solar radiation of 868 W/m² and liquid cooling was used.
Park et al. [79]	Crystalline silicon	Bismuth telluride	Experiment and simulation	16.30%	12.5%	30% optimized efficiency increase at 15 °C TE temperature difference.

Zhang et al. [151]	Polymer	Bismuth telluride	Experiment	N/A	N/A	Hybrid system power output increase of 46.6% compared to PV only system was observed.
Li et al. [81]	Crystalline silicon	N/A	Simulation	11.07%	9.5%	TE load resistance was 0.75Ω and figure of merit was 0.0085/K.
	GaAs	N/A	Simulation	22.94%	21.91%	TE load resistance was 1.60Ω and figure of merit was 0.0022/K
Zhang et al. [152]	Crystalline silicon	Nanostructured bismuth-antimony-telluride	Simulation	18.6%	18.4%	Concentration ratio was 16.
	Thin-film silicon		Simulation	14%	11%	Concentration ratio was 12.
	Polymer		Simulation	12%	4%	Concentration ratio was 5.
	CIGS		Simulation	23.5%	21.5%	Concentration ratio was 30.
Cui et al. [96]	Crystalline silicon	Bismuth telluride	Simulation	20.1%	N/A	Operating temperature was 300 K, optical concentration was 100 and PCM was used.
	CIGS	Bismuth telluride	Simulation	20.5%	N/A	Operating temperature was 300 K and optical concentration was 0.
	Single-junction GaAs	Bismuth telluride	Simulation	28.09%	N/A	Operating temperature was 425 K, figure of merit was 1.5, and optical concentration was 500.
	GaInP/InGaAs/Ge (III-V)	Bismuth telluride	Simulation	38.90%	N/A	Operating temperature was 300 K and optical concentration was 500.
Liao et al. [153]	Polycrystalline	Bismuth telluride	Simulation	15%	N/A	CG (Concentration ratio x Solar irradiance) was 875 W/m^2.
Chen et al. [154]	DSSC	N/A	Simulation	24.60%	N/A	Maximum power output of 1.389 mW was obtained.
Lin et al. [82]	Crystalline silicon	Bismuth telluride	Simulation	13%	10.24%	Power and efficiency enhancement of about 27% was observed.
Beeri et al. [155]	Multijunction	Bismuth telluride	Experiment and simulation	32.09%	32.08%	Concentration factor was 20 and hybrid power output was 0.190 W.
Da et al. [123]	GaAs	N/A	Simulation	18.51%	N/A	Figure of merit was 2.5 and Air Mass was 1.5.
Dou et al. [106]	DSSC	Bi_2Te_3/ZnO	Simulation	4.27%	N/A	Hybrid efficiency was 44.3% higher than efficiency of ZnO photoanode.
Attivissimo et al. [156]	Polycrystalline	Bismuth telluride	Simulation	N/A	N/A	TEG contributes about 12.2% to the hybrid system energy in Pachino.
Luo et al. [157]	Heterojunction	Bismuth telluride	Experiment	23.30% increase	N/A	Efficiency increase was achieved after 1 min illumination.
Pang et al. [158]	Monocrystalline silicon	Bismuth telluride	Simulation	5.9%	5.7%	Efficiency increase of 3.9% was observed.
Cotfas et al. [159]	Monocrystalline silicon	Bismuth telluride	Simulation	N/A	18.93%	Solar irradiance was 920 W/m^2.
	Polycrystalline silicon	Bismuth telluride	Simulation	N/A	16.71%	Solar irradiance was 1020 W/m^2.
	Amorphous silicon	Bismuth telluride	Simulation	N/A	2.88%	Solar irradiance was 720 W/m^2.
Lamba et al. [75]	Monocrystalline silicon	Bismuth telluride	Simulation	5.8%	5.2%	Number of TEG was 127 and concentration ratio was 3.
Zhu et al. [74]	Monocrystalline silicon	N/A	Experiment and simulation	23%	19%	TEG contributed extra electrical energy of 648 J during zero solar radiation period.
Hashim et al. [90]	Amorphous silicon	Bismuth telluride	Simulation	10.2%	N/A	Hybrid system power output increased to 163 mW.
Kossyvakis et al. [92]	Polycrystalline silicon	Bismuth telluride	Experiment and simulation	22.5% increase	N/A	Hybrid system efficiency was obtained theoretically.
	DSSC	Bismuth telluride	Experiment and simulation	30.2% increase	N/A	Hybrid system efficiency was obtained theoretically.
Zhang et al. [111]	Perovskite	Bismuth telluride	Simulation	18.6%	17.8%	Solar selective absorber was used.
Cui et al. [97]	Single-junction GaAs	Bismuth telluride	Experiment	13.45%	13.43%	Phase change material (PCM) was used.
Zhou et al. [160]	DSSC	p-type $Bi_{0.4}Sb_{1.6}Te_3$, n-type	Experiment	9.08%	7.21%	Hybrid efficiency was greater than TEG efficiency by 725.5%.

		$Bi_{2.85}Se_{0.15}Te_3$				
Lamba et al. [76]	Monocrystalline silicon	Bismuth telluride	Simulation	7.44%	7.068%	Maximum power output of the hybrid system was 595.5 mW.
Dallan et al. [114]	Monocrystalline silicon	Bismuth telluride	Experiment	13.2%	8.052%	PV and TE power output were 60.5 W/m² and 0.01 W/m² respectively.
Kil et al. [161]	Single junction GaAs	Bismuth telluride	Experiment	23.2%	22.5%	Solar concentration was 50 suns.
Soltani et al. [103]	Crystalline silicon	Bismuth telluride	Experiment	3.355% increase	N/A	SiO_2/water nanofluid cooling was used and power output was increase by 8.26% compared to natural cooling.
Li et al. [162]	CIGS	Bismuth telluride	Simulation	21.6%	20.71%	Concentration ratio was 200.
	Thin film silicon	Bismuth telluride	Simulation	13.1%	12.89%	Concentration ratio was 200.
	Polymer	Bismuth telluride	Simulation	8%	7.47%	Concentration ratio was 180.
Contento et al. [43]	Amorphous silicon	Nanostructured Bi_2Te_3	Simulation	≈57% increase	N/A	≈57% increase and ≈42% for directly and indirectly coupled systems respectively.
	Heterojunction CZTS	Nanostructured Bi_2Te_3	Simulation	≈35% increase	N/A	≈35% increase and ≈24% for directly and indirectly coupled systems respectively.
Liu et al. [163]	Perovskite	Bismuth telluride	Experiment	22.2%	9.88%	Ice bath was used for TE cooling and Air mass was 1.5.
Zhang et al. [164]	Silicon	N/A	Experiment	N/A	N/A	Hybrid system achieved high absorption for wavelengths of 0.3–1.1 μm.
Machrafi et al. [165]	Monocrystalline silicon	p-Sb_2Te_3 n-Bi_2Se_3	Simulation	25%	N/A	Thermoelectric nanoparticles were used, and optimum cooling velocity was 10 m/s.
Jeyashree et al. [166]	Polycrystalline silicon	Bismuth telluride	Experiment	N/A	N/A	Ice block was used for TEG cooling and hybrid system power output was 10.772 W.
Nishijima et al. [167]	Black silicon	N/A	Simulation	N/A	N/A	Ge__Sn layer was added to the solar cell and voltage increase of 7% was observed.
Babu et al. [68]	Polycrystalline	Bismuth telluride	Simulation	6% increase	N/A	TEG contributed energy of 1–3% of PV rating.
Li et al. [168]	InGaP/InGaAs/Ge triple-junction	Bismuth telluride	Experiment	33.53%	32.86	PCM and water cooling were used. Average efficiency was considered.

4.3 PV/TEG study type

Recently, there has been an increasing number of research works published relating to PV/TEG due to the high level of interest in such hybrid systems and its huge potential for enhanced performance compared to PV only systems. Some of the most recently published works on PV/TEG as at the time of writing this review are discussed in this section based on the type of study conducted. Generally, hybrid PV/TEG is usually studied experimentally or theoretically. The theoretical study also involves computational/numerical study.

4.3.1 Experimental study

Mahmoudinezhad et al. [59] presented an experimental study of the transient behaviour of a hybrid concentrating triple junction solar cell-thermoelectric generator system. A solar simulator was used in the experimental study to vary the concentrated solar radiations between 0 and 39 suns. The main objective of the research was to obtain the transient temperatures of the concentrating triple-junction solar cell and the hot and cold sides of the thermoelectric generator in addition to the short circuit current, open circuit voltage and maximum power outputs. Results obtained showed that the use of thermoelectric generator in a hybrid system is an effective way to stabilize the overall power output of the hybrid system. In addition, the authors argued that geometry can material optimization are two effective ways to enhance the contribution of the thermoelectric generator to the overall hybrid system power output.

Yin et al. [60] performed an experimental investigation on the feasibility of a concentrated photovoltaic-thermoelectric system with phase change material (PCM) and the thermal resistance analysis of such hybrid system. An experimental comparison of the performance of concentrated photovoltaic system, conventional concentrated photovoltaic-thermoelectric system and a concentrated photovoltaic-phase change material-thermoelectric (CPV-PCM-TE) hybrid system was presented. Furthermore, the performance of three hybrid CPV-PCM-TE systems using different PCM plates including paraffin with fins, paraffin/expanded graphite composite with fins and paraffin/copper foam composite were compared to study and analyse the PCM thermal resistance effect. Results obtained showed that the phase change material efficiently maintained the temperature of the PV cell in the hybrid CPV-PCM-TE to about 50 °C while the PV temperature in the hybrid CPV-TE system attained a high value of 80 °C. In addition, the results showed that the average power output of the hybrid CPV-PCM-TE system increased by 23.52% compared to that of the hybrid CPV-TE

system. Furthermore, the authors argued that the cooling system thermal resistance had a little influence on the PV cell due to the presence of the PCM which controlled the temperature.

The feasibility and optimization of a hybrid PV/TEG system was studied experimentally by Lekbir et al. [61]. The experimental study was carried out in a laboratory and a monocrystalline silicon solar cell was used. Results from the experiment carried out showed that the maximum power output of the hybrid system was 0.12 W and this was greater than that of the PV cell and TEG therefore, the hybrid system performed better under the same environmental conditions. Marandi et al. [62] performed an experimental investigation of a hybrid PV/TEG system with a solar cavity receiver. A novel method to reduce re-radiation from PV panels by using cavity receiver was presented and the developed cavity hybrid PV/TEG system achieved a peak efficiency of 21.9%. Zhang et al. [63] presented a unique structural arrangement for enhanced performance of hybrid PV/TEG system. In the design, ceramic plates on the TE module were eliminated to enhance heat transfer by reducing thermal resistance and a V-type groove was used to enhance absorption of solar energy by keeping each PV cell in a perpendicular position to its adjacent PV cells. The authors performed an experimental investigation and found that the new TE structure enhanced the performance of the hybrid system. Some of the other experimental papers on hybrid PV/TEG system can be seen under the column 'study type' in Tables 4 and 5 with their corresponding performance data.

4.3.2 Theoretical/computational study

Rodrigo et al. [64] presented a theoretical study on the performance and economic limits of passively cooled hybrid PV/TEG systems. The novelty of this study was the development of an electric/thermal/economic model to investigate the performance and economic limits obtainable with passive cooling of a concentrated hybrid PV/TEG system. In addition, the developed model allowed the area of the thermoelectric generator to be adjusted. Results obtained showed that the optimization of the thermoelectric generator area is essential for keeping the cell operating temperature within acceptable limits. Furthermore, an avant-garde mathematical model was presented in the study and a three-dimensional model of the concentrator photovoltaic-thermoelectric receiver was developed based on finite element method. The authors argued that the newly proposed passive cooling concept would influence the development of future passively cooled concentrated PV/TEG prototypes.

A detailed parametric study on the performance of a hybrid PV/TEG system using numerical simulation was performed by Lakeh et al. [65]. In the study, the effect of ambient conditions, cold side temperature and load resistance of the thermoelectric generator on the performance of the hybrid system was considered. Furthermore, the material properties, number of thermoelectric generator couple, cross sectional area and length of the system were determined in the optimum range so as to optimize the performance of the hybrid system. Results obtained showed that the electrical performance of the hybrid system in terms of maximum power output was highly dependent on the geometrical characteristics of the device. Also, the numerical simulation results showed that the hybrid PV/TEG system had a higher efficiency compared to the single solar cell.

Lekbir et al. [66] performed a numerical investigation of a nanofluid based concentrated photovoltaic/thermal-thermoelectric generator (CPV/T-TEG) hybrid system with a cooling channel. Compared to the nanofluid based CPV/T, CPV and CPV/TEG with heat sink, the proposed hybrid system electric energy was higher by 10%, 47/7% and 49.5% respectively. Lorenzi et al. [67] presented a model for determining the theoretical efficiency of a hybrid PV/TEG system for terrestrial application. The authors argued that there is an optimum operating temperature for obtaining maximum hybrid system efficiency and this temperature is not influenced by the TEG geometrical dimensions and number of legs. Efficiency increase of 4–5% compared to PV only system was observed for the hybrid system. Babu et al. [68] also performed a theoretical investigation of an unconcentrated hybrid PV/TEG system using the MATLAB/Simulink environment. It was found that the hybrid system had an overall efficiency increase of 6% and additional energy projection of 5%.

Motiei et al. [69] performed a numerical simulation of a hybrid PV/TEG system using an unsteady, two dimensional numerical model. The performance of the hybrid system was compared with that of a PV only system and it was found that in the hybrid system, the PV conversion efficiency and electrical power output increased by 0.59% and 5.06% respectively compared to the PV only system. However, it is worth noting that the Thomson effect was not considered in this study and temperature independent thermoelectric material properties were used. Similarly, Mahmoudinezhad et al. [70] studied the transient response of a hybrid CPV/TEG system. A numerical investigation was carried out using finite volume algorithm. The influence of thermal contact resistance at the interfaces between the CPV/TEG and TEG heat sink was studied and the influence of varying weather conditions on the performance of the hybrid system was investigated. The results showed that increase in thermal contact resistance leads to a decrease in efficiency of the TEG and CPV. Furthermore, the authors argued that the use of TEG in the hybrid system enabled the stable generation of power under varying weather condition.

A rare three-dimensional numerical simulation of a PV/TEG was performed by Fallan Kohan et al. [71]. The inner structural complexities were ignored in the numerical model and the hybrid system was considered as a homogeneous medium. Electric power output in the hybrid system was modelled as an internal energy sink and finite volume method was used for the numerical simulation. It was found that under certain environmental conditions, the hybrid PV/TEG system generated more power than the PV only system. The authors argued that the presence of the TEG could have a negative effect on the cooling of the PV. Zhou et al. [72] developed a Multiphysics coupling mathematical model for studying the performance of a hybrid PV/TEG system which consisted of an all-back-contact silicon PV with nanostructured surface, a thermoelectric device and a plane fin heat sink. It was found that the power output density of the PV/TEG increased by 9.1% due to the optimization of the hybrid system heat transfer structure. Under the column 'study type' in Tables 4 and 5, some of the other theoretical papers on hybrid PV/TEG system can be seen with their corresponding performance data.

5 Current research focus areas in hybrid PV/TEG

A plethora of studies on hybrid PV/TEG have been performed recently with each study addressing a particular area in the hybrid system research. This section presents some of the main research focus areas being explored by researchers on hybrid photovoltaic-thermoelectric generator and some niche applications of hybrid PV/TEG.

5.1 Concentrated hybrid system

Vorobiev et al. [73] presented a theoretical study of two different approaches for the thermal management of PV (Fig. 11). In the first approach, the unabsorbed solar radiations from the semiconductor material of the PV was concentrated on a thermoelectric

generator for further conversion into electrical energy thus, the PV operated at a low temperature. The second approach sees the PV cell operating at elevated temperatures while the thermoelectric generator is used to convert the excess heat. The only difference between both approaches is the position of the concentrator and PV. The basic elements of the systems shown in Fig. 11 are; Concentrator (CONC), PV cell (PVC), Thermoelectric Generator/High Temperature Stage (HTS) and the 2-axis Solar Tracking System (STS2). The authors found that using the first approach, the hybrid system obtained enhanced efficiency of 5–10% while the second approach didn't significantly improve the overall hybrid system efficiency. A drawback from this research is that, an assumed high ZT value was used which is not currently practical.

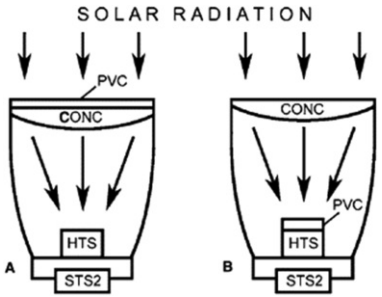

Fig. 11 Schematic diagram of PV/TEG with PV operating at (A) low and (B) high temperatures [73].

alt-text: Fig. 11

Zhu et al. [74] performed a detailed experimental and numerical investigation of the performance of a thermal concentrated hybrid PV/TEG system (Fig. 12). A copper plate operating as the thermal concentrator and conductor was sandwiched between the PV and TEG and it increased the temperature difference across the TEG. Finite element simulation software, ANSYS was used to study the temperature distribution and water cooling was applied to the hybrid system. It was observed that a large percentage of thermal loss is cause by air convection thus, transparent enclosure (Polymethyl methacrylate) and optimal thermal concentration were introduced into the designed system. Results obtained showed that the use of the copper plate enhanced temperature uniformity and the efficiency of the hybrid system was about 23%.

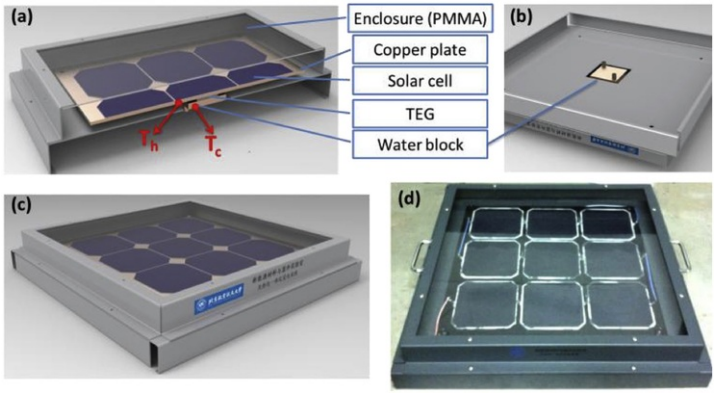

Fig. 12 Hybrid PV/TEG (a) cross-sectional view, (b) bottom view, (c) global view and (d) physical diagram [74].

alt-text: Fig. 12

Lamba et al. [75,76] performed a couple of investigations on concentrated PV/TEG systems. The influence of Thomson effect, concentration ratio, number of TEG, solar irradiance, PV current and TE current on the efficiency and power output of the hybrid system, PV and TEG only systems were studied [75]. Results obtained (Fig. 13) showed that the power output of the hybrid PV/TEG system decreases due to Thomson heating when the Thomson effect is considered in the TEG analysis. It was found that Thomson effect significantly reduces the hybrid system power output especially for highly concentrated systems [75]. Another theoretical investigation was carried out on the concentrated PV/TEG and the influence of TEG leg length, load resistance ratio, concentration ratio and fill factor on performance of the hybrid system were studied [76]. It was observed that the TEG contributes more to the total hybrid system power output when higher concentration ratios are used. In addition, the hybrid system obtained a maximum efficiency of 7.44% which was 5% higher than that of the PV only system [76].

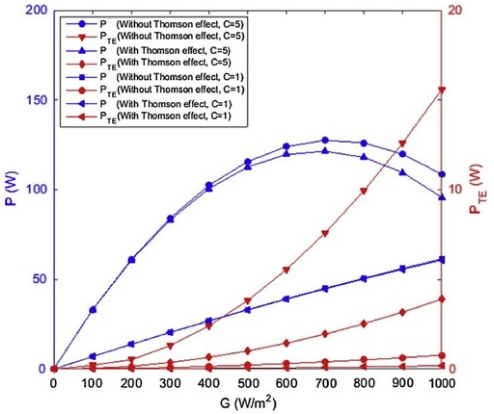

Fig. 13 Variation of hybrid PV/TEG and TEG system power output with solar irradiance [75].

alt-text: Fig. 13

An additional study on hybrid concentrated PV/TEG system was carried out by Rezania and Rosendahl [77]. The effect of the most important design parameters on the hybrid system performance were studied and it was observed that the concentrated photovoltaic-thermoelectric (CPV/TEG) system using the current available thermoelectric materials (ZT≈1) had a better conversion efficiency compared to the CPV only system (Fig. 14). Recently, Mahmoudinezhad et al. [78] performed a feasibility study of a hybrid CPV/TEG system for low solar concentrations (Fig. 15). An experimental and numerical investigation was carried out to study the performance of the hybrid system. The experiment was carried out using concentrated radiation from a solar simulator while finite volume method was used to perform the numerical simulation. The authors argued that the experimental results were in agreement with the simulation results. It was found via the experiment that the maximum and minimum efficiency of the CPV were 35.33% and 23.02% respectively.

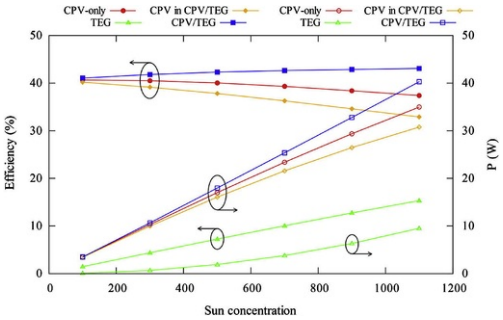

Fig. 14 Variation of system efficiency with sun concentration [77].

alt-text: Fig. 14

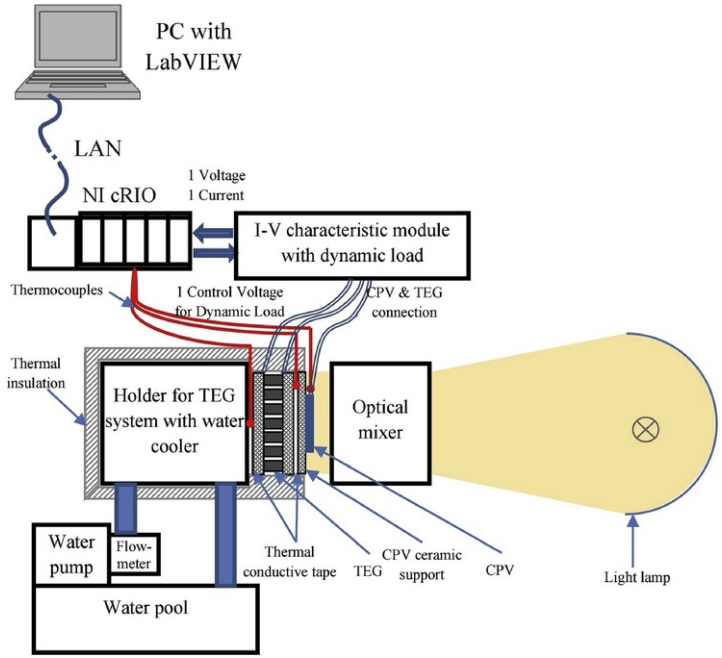

Fig. 15 Schematic diagram of experimental PV/TEG setup [78].

alt-text: Fig. 15

5.2 Hybrid system coupling

Effective coupling of the photovoltaic and thermoelectric systems can enhance the performance of the hybrid system and reduce losses. In fact, it is essential to perform a lossless matching of the two different systems (PV and TE) to obtain optimized efficiency results. In addition, a TEG possesses an internal resistance which must be adequately matched with that of the PV so as the ensure the hybrid system performance is not worse than that of the individual systems.

Park et al. [79] performed the optimization of a hybrid PV-TEG system via lossless coupling and observed an efficiency enhancement of about 30% in the hybrid system compared to the conventional PV system. The achieved lossless coupling enabled the hybrid system power output to be equal to the sum of the power output from the individual systems (PV and TE). In addition, the authors argued that proper selection of the internal resistance and TE elements number was essential to obtaining fill factor (FF) and voltage gains. In addition, Lorenzi et al. [80] analysed the effect of several parameters on the power output of an electrical coupled PV/TEG system. Results obtained showed that for solar cells with a small series resistance, the voltage needed for electrical lossless coupling was smaller. In addition, it was found that lossless conditions strong depend on temperature.

Load resistance matching is another optimization technique to enhance the performance of the hybrid system. Successfully matching the internal resistance of the hybrid system with the external load resistance would ensure maximum power output is obtained. Li et al. [81] studied the inconsistent phenomenon of the thermoelectric load resistance in PV/TEG systems. Two different PV cells were used in the analysis and the thermoelectric load resistances for obtaining maximum power output in the TE only system and PV/TEG system were determined. The main argument of the authors was that the load resistance at which maximum power output could be obtained from a thermoelectric generator might be different from the optimum thermoelectric load resistance in a hybrid PV/TEG system. Therefore, they performed a series of investigations with the aim of studying this inconsistent load resistance effect. In addition, thermal contact resistance between the PV and TEG, TEG and heat sink were considered in the simulations. The effect of concentration ratio, wind speed and ambient temperature were investigated. Results obtained showed that the thermoelectric load resistance for maximum power output from the TEG alone, TEG in PV/TEG and PV/TEG are entirely different. Therefore, the authors concluded that using the optimum TE load resistance in a TEG only system for the analysis of a PV/TEG system would cause errors and prevent the attainment of hybrid system maximum power output.

Lin et al. [82] performed a similar research to Ref. [81] on hybrid PV/TEG load resistance matching. Thermodynamic method was used to investigate the optimum performance characteristics of the hybrid system and problems relating to load matching in practical hybrid system design were discussed. Results obtained showed that the maximum power output and maximum efficiency of the hybrid system could be obtained at the same operating current (Fig. 16). In addition, hybrid system efficiency and power output of about 27% compared to the PV only system were observed. Finally, the authors argued that the use of thermoelectric material with a figure of merit ($Z = 0.004/K$) could lead to the hybrid system efficiency enhancement of about 30%.

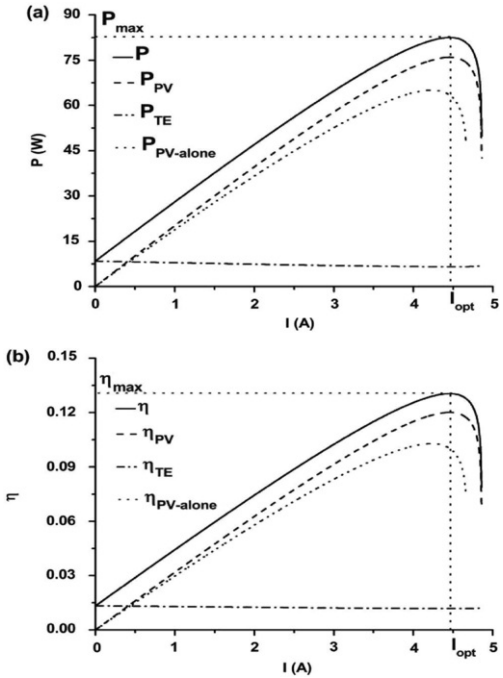

Fig. 16 Hybrid system and PV only system (a) power output and (b) efficiency [82].

alt-text: Fig. 16

The potential negative effect of PV/TEG coupling was presented by Lin et al. [83]. The authors placed emphasis on the coupling between discretized nodal temperatures and the hybrid system electrical power output. A modified Newton-Raphson method which involved two computational stages was used to solve the modelling equations. The authors argued that their method reduced computational efforts in terms of solving algebraic manipulations and coding as well as, making debugging of the code easier when divergence occurs. Results obtained showed that for the specific parametric values chosen, the efficiency of the hybrid system was lower than that of the PV only system (Fig. 17). It is therefore imperative to properly couple the PV/TEG for achievement of enhanced overall efficiency rather than reduced efficiency when compared to the PV only system.

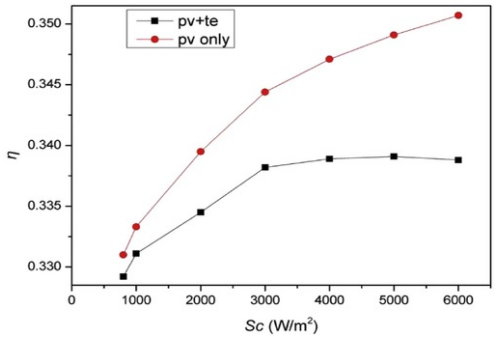

Fig. 17 Variation of hybrid system and PV only system efficiency with solar radiation [83].

alt-text: Fig. 17

Similar to Ref. [83], Bjørk et al. [84] observed a negative effect of hybrid system coupling due to the reduced performance of the hybrid system compared to the PV only system. An analytical investigation was carried out using four different PV cell types including, crystalline silicon (c-Si), amorphous silicon (a-Si), copper indium gallium selenide (CIGS) and cadmium telluride (CdTe). Bismuth telluride thermoelectric material with a maximum operating temperature of 200 °C was used in the analysis. The authors found that only the

hybrid system with amorphous silicon had an enhanced efficiency and power output compared to the PV only system. Contrarily, the hybrid system with the other types of PV considered had a worse performance than the PV only system (Fig. 18). The explanation for this trend was that the PV performance degradation with increased temperature was much greater than the TEG power production due to the low efficiency of the TEG. Consequently, the authors argued that coupling of photovoltaic and thermoelectric is not a viable option for power production due to the decrease in PV performance as temperature increased.

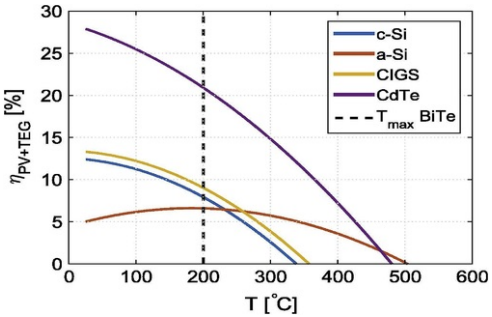

Fig. 18 Hybrid system efficiency variation with temperature for different PV cells [84].

alt-text: Fig. 18

Hajji et al. [85] deviated from the norm by presenting an indirect coupling of a hybrid PV/TEG system (Fig. 19). A combination of finite element method and MATLAB/Simulink software was used to perform the numerical simulations and a comparison between the directly coupled and indirectly coupled systems was presented. Basically, in the directly coupled system, all the components were physically connected while for the indirect coupling, the optical concentrator had no direct physical contact with the PV and TEG. The developed system was properly insulated to reduce heat loss and it was observed that the indirect coupling method significantly improved the hybrid system overall efficiency.

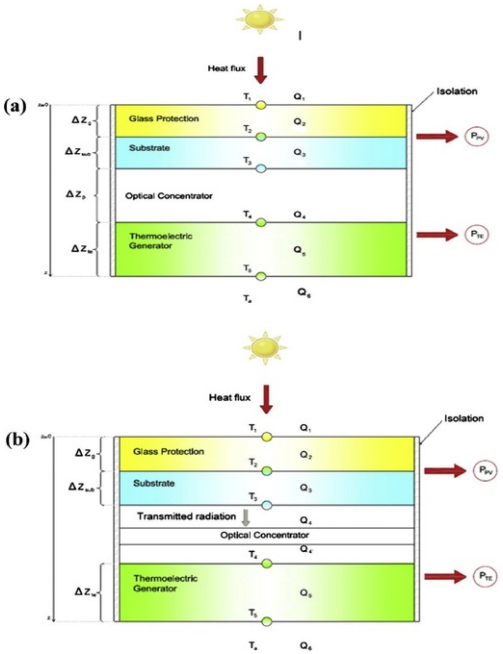

Fig. 19 Schematic of PV/TEG system for (a) direct and (b) indirect coupling [85].

alt-text: Fig. 19

Adopting a similar approach as [85], Contento et al. [43] investigated the performance of an optically coupled (indirect) PV/TEG system using a vacuum-sealed compound parabolic concentrator and a thermally coupled (direct) PV/TEG system (Fig. 20). Two types of PV cells were considered including, single junction amorphous silicon and heterojunction Cu_2ZnSnS_4 (CZTS). Results obtained showed that direct coupling of hybrid PV/TEG system enables the achievement of large conversion efficiency while indirect coupling reduces the temperature of the PV thus, improving its reliability and lifespan. In addition, the authors observed the efficiency improvement in the directly coupled hybrid system to be ≈ 57% and ≈35% for the amorphous silicon and CZTS respectively. While for the indirectly coupled hybrid system, the efficiency improvement was ≈42% and ≈24% for the amorphous silicon and CZTS respectively.

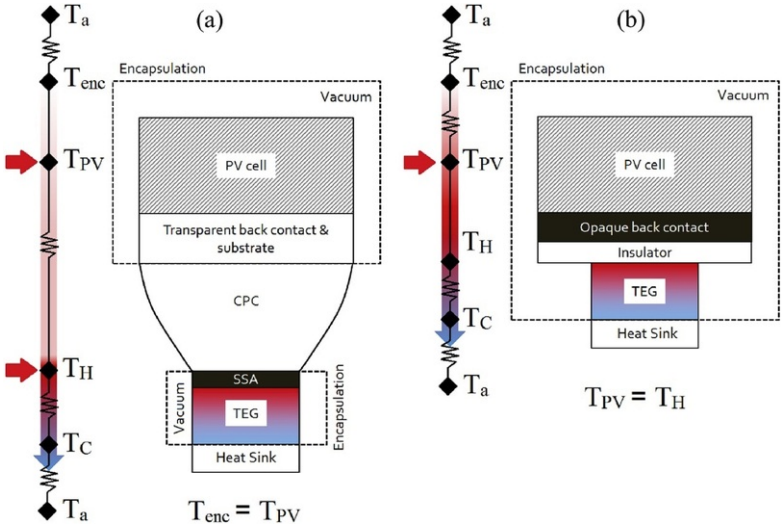

Fig. 20 Schematic of developed hybrid system with (a) indirect and (b) direct coupling [43].

alt-text: Fig. 20

5.3 Thermoelectric geometry optimization

The geometry of a thermoelectric generator significantly affects its performance therefore, several research [86–89] on optimization of TEG geometry has been carried out. However, the integration of thermoelectric generators into PV necessitates the investigation of the optimum geometry of the TEG in the hybrid PV/TEG system as this may differ from the optimum geometry in the TEG only system.

Hashim et al. [90] developed a numerical model for the optimization of thermoelectric generators in a hybrid PV/TEG system. The model could efficiently determine the optimum TEG geometry for maximum hybrid system power output. In this study, passive water and copper plate were used as the cooling system and thermal concentrator respectively. The authors argued that the geometry of the TEG in a hybrid system influences the overall power output of the system as it determines the solar cell operating temperature and TEG temperature difference. It was also found that the power output of TEG modules with a smaller cross-sectional area than that of the PV was higher than those with a larger cross-sectional area. Finally, it was observed that operating the hybrid system in vacuum could enhance its performance.

Recently, Shittu et al. [91] performed a significant study on the optimum thermoelectric generator geometry in a hybrid PV/TEG system for enhanced overall efficiency. The authors optimized the two geometry area ratios $(R_A = A_H/A_C)$ and $(R_S = A_n/A_p)$ of a thermoelectric generator. Two different PV types (Cell A and Cell B) with different reference efficiency and temperature coefficient value were studied and the influence of TEG geometric parameters, solar irradiation and concentration ratio on the hybrid system efficiency were investigated. COMSOL Multiphysics was used to perform the finite element numerical simulations and temperature dependent thermoelectric properties were used. Results obtained (Fig. 21) showed that the optimum geometry of the TEG in a hybrid system is highly dependent on the type of solar cell used.

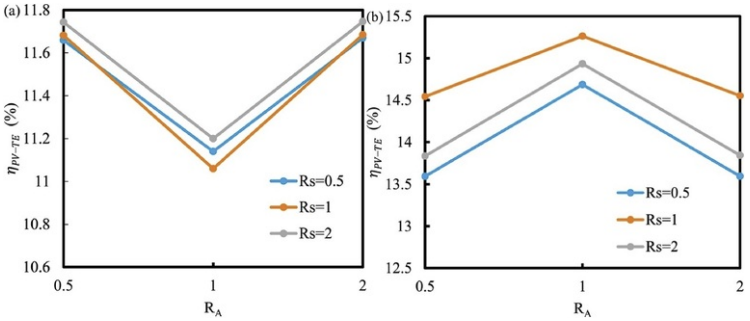

Fig. 21 Hybrid system efficiency variation with geometry area ratio for (a) solar cell A and (b) solar cell [91].

alt-text: Fig. 21

Kossyvakis et al. [92] investigated the influence of TEG geometry on the performance of a hybrid PV/TEG system using two different PV cell types (polycrystalline and dye-sensitized). An experimental and numerical study was carried out on four-wire and two-wire hybrid PV/TEG systems and water cooling was used. Results obtained showed that the use of thermoelectric generator with short leg length is favourable for hybrid system power output enhancement under sufficient illumination because it can reduce the operating temperature of the PV cell. This observation is significant because it can reduce the hybrid system manufacturing costs because less thermoelectric material will be used to achieve high overall power output.

More TEG geometry optimization efforts in hybrid PV/TEG were carried out by Li et al. [93,94]. The authors argued that the PV and TE systems have a complex relationship in the hybrid configuration therefore, the optimization of TEG alone would not be sufficient for obtaining maximum power output and efficiency from the hybrid system [93]. Furthermore, the primary constraints of a hybrid PV/TEG system were investigated and the influence of TEG geometry parameters, cold side temperature and solar irradiance on the performance of the hybrid system were studied. It was found that the overall efficiency of the hybrid system increased as the cross-sectional area of the TEG increased and shorter TEG leg length is favourable [94].

5.4 Energy storage

Due to the intermittent nature of solar radiations, it is sometimes necessary to add an energy storage unit to the hybrid PV/TEG system. The storage unit can help store thermal energy for use during periods of low solar radiation. Li et al. [95] investigated the perform of a hybrid PV/TEG system with an energy storage unit (Fig. 22). The thermal energy which was stored in the energy storage unit was used as the heat source for the TEG hot side. The authors argued that it is essential to store thermal energy for both heating and cooling reservoirs using phase change materials (PCMs) so as to maintain stable PV and TE operating temperatures. In addition, they recommended the use of inorganic eutectic salt mixtures as PCMs for moderate to high temperature thermal energy storage. While for high grade cold storage applications, PCM eutectic solutions were recommended due to their ability to storage thermal energy down to 159 K. The results obtained showed an overall hybrid system efficiency enhancement of about 31–34% using thermoelectric materials with ZT = 1 (see Fig. 24) (see Fig. 23).

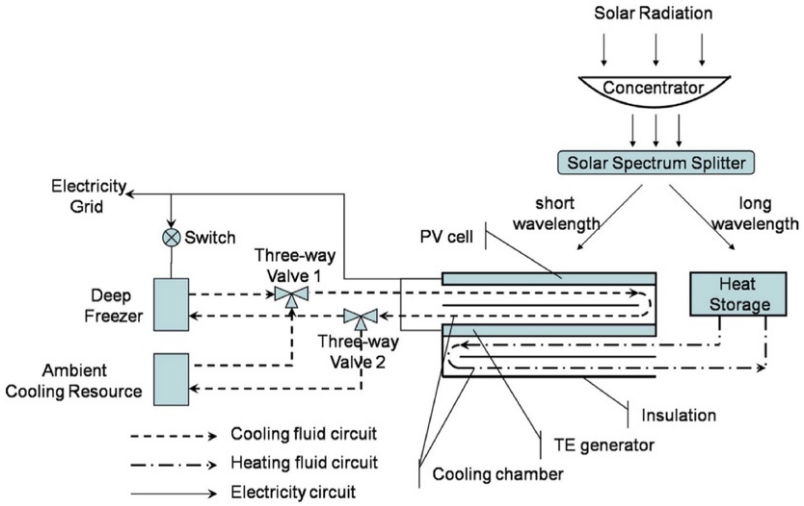

Fig. 22 Schematic of PV/TEG system with heat storage unit [95].

alt-text: Fig. 22

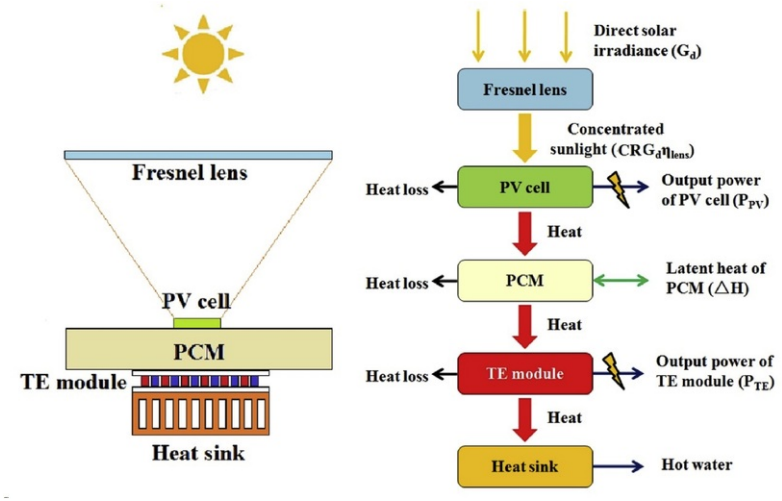

Fig. 23 Schematic diagram and energy flow of the hybrid PV-PCM-TE system [97].

alt-text: Fig. 23

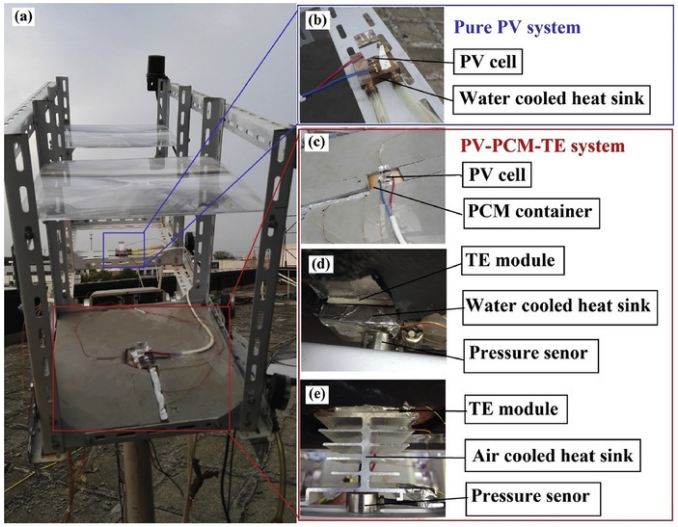

Fig. 24 (a) Hybrid PV-PCM-TE system and PV only system, (b) PV only system, (c) top view of hybrid PV-PCM-TE, (d) bottom view of hybrid system with water heat sink and (3) bottom view of hybrid system with air heat sink [97].

alt-text: Fig. 24

Similarly, Cui et al. [96] studied the performance of a novel PV-PCM-TE system in which the PCM was used to mitigate the temperature fluctuations in the hybrid system thus, enabling the hybrid system to operate at fixed conditions. The advantage of using a PCM is that it can absorb a large amount of energy as latent heat at a constant phase transition. Four PV types were investigated for the PV only, PV/TE and PV-PCM-TE systems and the significance of incorporating the PCM into the hybrid PV/TE system was investigated under fluctuating solar radiation. The PCM tank was attached directly below the PV cell to reduce the thermal contact resistance and difference in temperature between the PV and PCM. The authors recommended the use of paraffin PCM when the PV-PCM-

TE is operated at a temperature below 375 K. However, for temperatures above 420 K, NaOH

KOH PCM was recommended. Results obtained from this research showed that the PV-PCM-TE had a better performance compared to PV only and/or PV/TE systems.

Subsequent to the theoretical investigation carried out by Ref. [96], the same authors (Cui et al.) carried out the experimental investigation of the proposed novel hybrid PV-PCM-TE system [97]. The schematic diagram and experimental realisation of the system are shown in Figs. 21 and 22 (Please change these to Figs. 23 and 24) respectively. The main novelty of this study is the introduction of phase change material (PCM) into the hybrid PV/TEG system to maintain the system operating temperature. Influence of optical concentration ratio and cooling system on the performance of the hybrid system were studied. In addition, a comparison between the novel hybrid system and PV only system was made. It was observed that the novel hybrid system had a higher efficiency compared to the PV only system due to the use of phase change material.

5.5 Thermoelectric generator cooling

Adopting a similar approach used by Ref. [73], Willars-Rodríguez et al. [98] performed an experimental investigation of a hybrid PV/TEG (Fig. 25). The PV cells were operated in a cold area (≤310 K) while the cooling unit and the TEG were operated in a high temperature area (≤500 K). The reason for this arrangement is because the PV performs better at lower temperatures while the TEG requires high temperature for high performance thus, their separation into two areas (cold and hot) would enhance the performance. In addition, the TEG was cooled using the thermosiphon effect of running water while the hybrid system generated thermal energy was stored in the water tank. The authors performed finite element simulation of the thermoelectric generator cooling unit and the result obtained is shown in Fig. 26. The assumption considered was that solar radiation is applied directly to the copper plate and it was found that the maximum temperature of the plate was 350 °C while the inlet and outlet water temperatures were 25 °C and 45 °C respectively. Results obtained showed that the hybrid system generated an electric power of 7 W and thermal power of 30 W.

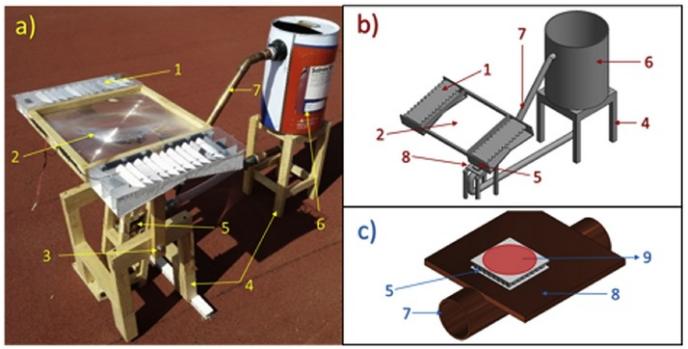

Fig. 25 (a) Hybrid system experimental test rig, (b) hybrid system schematic representation and (c) integrated thermoelectric generator with cooling unit. Where: (1) PV mounted on cooling system, (2) Fresnel lens, (3) solar tracker, (4) structural elements, (5) TEG, (6) storage tank, (7) pipe, (8) heat sink and (9) thermal incider spot [98].

alt-text: Fig. 25

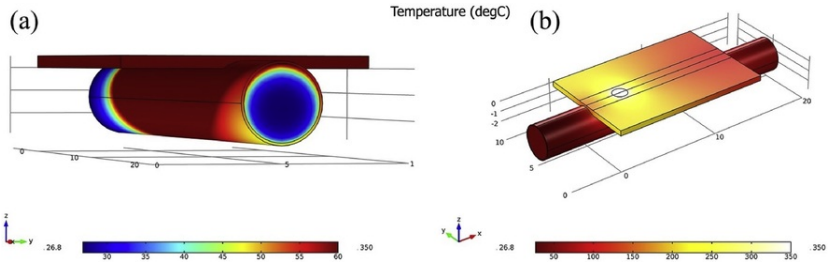

Fig. 26 Temperature distribution in thermoelectric generator cooling unit (a) running water tube and (b) copper plate [98].

alt-text: Fig. 26

Yin et al. [99] investigated the performance of a hybrid PV/TEG system using three different cooling methods (Fig. 27). Natural cooling, forced air cooling and water cooling were compared and the influence of optical concentration ratio, water velocity and thermal contact resistance were studied. In addition, the hybrid systems using four different PV types including, monocrystalline silicon, polycrystalline silicon, amorphous silicon and polymer cell were investigated to determine the best performing PV. Results obtained showed

that a reduction in the cooling system thermal resistance could lead to enhanced heat flux to the TEG thus, improving its total power output. The effect of the cooling system on the performance of the hybrid system with different PV cells is shown in Fig. 28. It is obvious that natural cooling (free cooling) is not suitable for concentrated hybrid systems due to its inferior performance compared to the other cooling methods. In addition, Fig. 28 shows that water cooling is more effective for hybrid systems than natural cooling and forced air cooling. Therefore, the authors concluded that water cooling is the most suitable cooling method for hybrid PV/TEG systems especially highly concentrated systems. In addition, they argued that crystalline silicon and polycrystalline silicon PV are not suitable for hybrid PV/TEG systems because of their reduced overall efficiency compared to the PV only system.

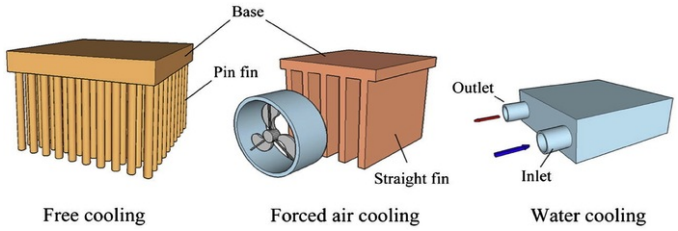

Fig. 27 Different types of thermoelectric generator cooling systems [99].

alt-text: Fig. 27

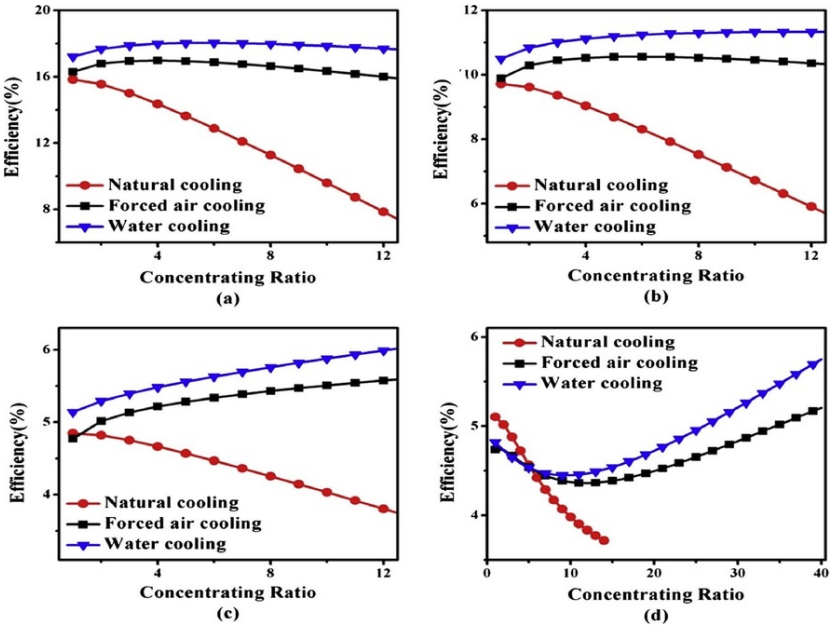

Fig. 28 Hybrid system overall efficiency variation with concentration ratio for (a) crystalline silicon cell, (b) polycrystalline silicon cell, (c) amorphous silicon cell and (d) polymer cell [99]. (For interpretation of the references to colour in this figure legend, the reader is referred to the Web version of this article.)

alt-text: Fig. 28

Adopting a similar research objective as [99], Zhang et al. [100] carried out a thermal resistance analysis of a concentrated PV/TEG system. A three-dimensional numerical simulation was used to study the temperature distribution and power output of the hybrid system. In addition, the influence of cooling system, thermal resistance and concentration were studied. Water and air cooling were applied to the hybrid system and the performance of the system was observed. It was observed that the insertion of a copper plate between the PV and TE can decrease the thermal resistance between the systems as the copper plate improves the temperature uniformity and this is in agreement with [74]. Furthermore, the authors argued that the natural convection and radiation do not affect the performance of highly concentrated PV/TEG systems. In addition, it was observed that a decrease in the PV cell area leads to an increase in the hybrid system efficiency. Finally, water cooling was observed to be more suitable for highly concentrated PV/TEG systems compared to air cooling. This finding is in agreement with [99].

Pang et al. [101] investigated experimentally, the significance of heat sinks in a hybrid PV/TEG system. Two heat sink structures (Pin fin and Plate fin) were investigated to determine which one had a better cooling effect on the hybrid system. Also, the hybrid

system with and without heat sinks were compared to show the significance of the heat sink. Results obtained showed that the heat sink with natural convection cooled the PV/TE system by 8.29 °C which was 1.8 °C greater than that of the PV only system. However, the authors argued that the integration of thermoelectric into PV, amplified the fluctuation of the cooling performance of the hybrid system with heat sink.

Compared to the conventional cooling methods like water and air, nanofluid was proposed as a more efficient cooling method for hybrid PV/TEG by Wu et al. [102]. The authors used a theoretical approach to investigate the performance of glazed and unglazed PV/TEG systems. The effect of thermoelectric figure of merit, concentration ratio, wind velocity and nanofluid flow rate were studied. It was found that the efficiency of unglazed PV/TEG is higher than that of the glazed PV/TEG when figure of merit Z = 0.0021/K. In addition, the authors argued that some large figure of merit values may not improve the performance of the hybrid system. Similar to the observation from Ref. [81], it was found that the optimum load resistance for maximum TEG efficiency and PV/TEG efficiency are different. Finally, the results obtained showed that nanofluid cooling enhances the performance of PV/TEG systems compared to water cooling especially for the glazed system (Fig. 29).

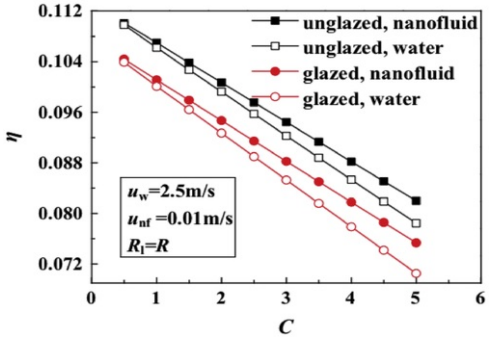

Fig. 29 Variation of hybrid system efficiency with concentration ratio for different cooling systems [102].

alt-text: Fig. 29

Soltani et al. [103] investigated a new nanofluid-based cooling system for enhancing the performance of hybrid PV/TEG systems and an experimental comparison with conventional cooling systems was presented. Five different cooling methods were investigated including, natural cooling, forced air cooling, water cooling, SiO_2/water nanofluid cooling and Fe_3O_4/water nanofluid cooling. The results obtained in terms of efficiency and power output enhancement are shown in Table 3. Mean relative error (MRE) statistical error analysis was used to calculate the performance enhancement relative to the natural cooling system. It was found that the performance of the TEG was mainly affected by the cooling system while the PV cell's temperature was also influenced by the cooling system. The authors argued that nanofluid cooling performed better especially SiO_2/water nanofluid cooling which enhanced the efficiency and power output of the hybrid system by 3355% and 8.26% respectively compared to the natural cooling.

5.6 New generation PV and TE materials

Guo et al. [104] compared the performance of a four-wire and two-wire hybrid PV/TEG system with dye-sensitized solar cell (DSSC). This study is similar to Ref. [92] where a four-wire and two-wire PV/TEG system were also investigated. Considering the two-wire system, the authors found that proper matching the TE and PV output currents can enhance the efficiency of the hybrid system by 10% compared to a single dye-sensitized solar cell. Similarly, Wang et al. [105] integrated a series-connected dye-sensitized solar cell with a solar selective absorber (SSA) and a thermoelectric generator as a proof of concept for a hybrid system. The system obtained an overall conversion efficiency of 13.8% and maximum power output of 13.8 mW/cm^2 under a solar irradiance of 100 mW/cm^2 and Air Mass of 1.5G. The authors argued that the conversion efficiency of the hybrid system could be enhanced further by optimizing the system.

Dou et al. [106] fabricated a novel photoanode architecture by integrating a Bi_2Te_3 nanotubes with Zinc oxide (ZnO) nanoparticles (Fig. 30) to improve the performance of a dye-sensitized solar cell. The Bi_2Te_3 nanotubes were synthesized using a two-step solution phase reaction and it was observed that the nanotubes accelerated the electron transport process in photoanode, increased the lifespan of the electrons and enhanced the electron collection efficiency. The authors found the highest efficiency of the novel hybrid system composed of DSCC and Bi_2Te_3 (1.5 wt%) to be 4.27% which was 44.3% higher than that of a single ZnO photoanode.

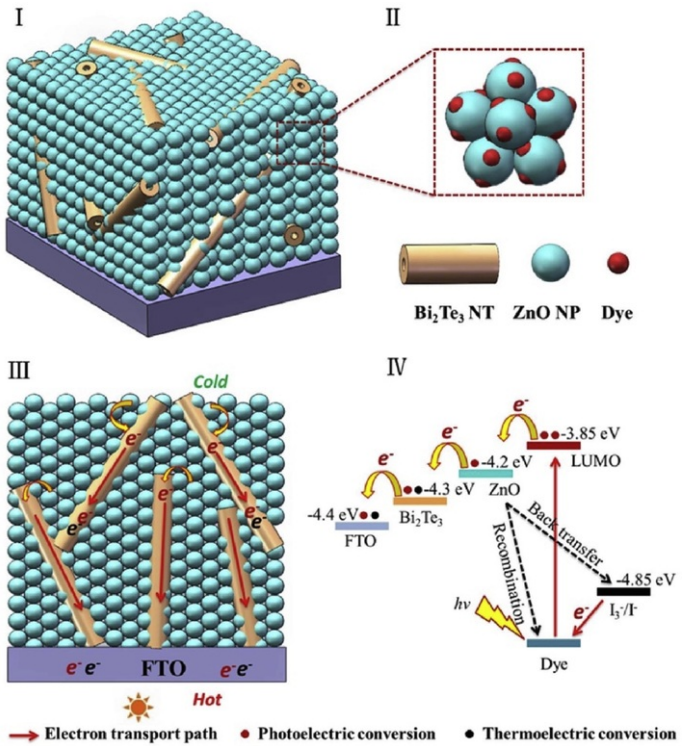

Fig. 30 Schematic diagram of Bi_2Te_3/ZnO composite photoanode (I, II) electron transport process, (III, IV) energy diagram of system operation [106].

alt-text: Fig. 30

Increasing the solar radiation absorptivity of a hybrid system can significantly enhance its efficiency. Rai et al. [107] developed a methodology to enhance the performance of a hybrid PV/TEG system by using a fishnet metamaterial structure which could increase the solar radiation absorptivity of the hybrid system. A planar fishnet structure was included in the back-passivation layer of the solar cell for enhanced absorptivity of radiations close to the infrared band of the solar spectrum. The fishnet structure is capable of accumulating electromagnetic radiation by using its rectangular cells as a resonant circuit and it was fabricated by e-beam lithography assisted lift-off technique. In addition, nanoporous Bi_2Te_3 and Sb_2Te_3 particles were synthesized and used as the p-type and n-type thermoelectric materials respectively. The fabrication process for the fishnet metamaterial structure using nanoimprinting and die transfer for p-type and n-type thermoelectric materials is shown in Fig. 31. Results obtained showed that the hybrid system with fishnet structure had an enhanced efficiency around 11 folds.

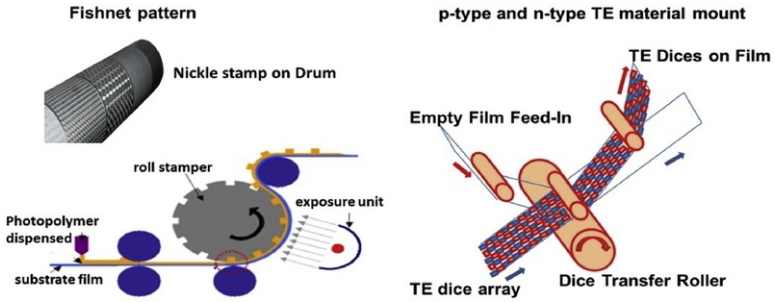

Fig. 31 Fabrication process for fishnet metamaterial structure [107].

alt-text: Fig. 31

Adopting the same method as [107], Oh et al. [108] investigated the performance of a hybrid PV/TEG system with fishnet structure (Fig. 32). The authors argued that the fishnet geometry and material properties are important parameters that determine the performance of the system therefore, optimization of the fishnet structure was carried out using parametric simulation. The pitch, width and thickness of the fishnet structure were optimized using numerical simulation approach. A slight improvement in the results obtained from Ref. [107] was observed by the authors [108] as the optimized hybrid system with fishnet structure had an enhanced efficiency around 12 folds compared to the system without fishnet.

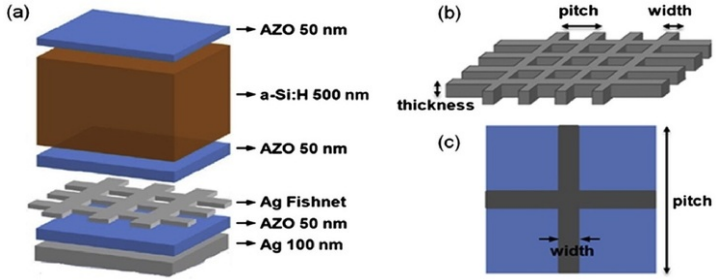

Fig. 32 Schematic diagram of hybrid stem with fishnet. (a) 3D schematic of thin film solar cell, (b) fishnet structural parameters and (c) top view of solar cell [108].

alt-text: Fig. 32

Xu et al. [109] presented a unique method for photon management in full spectrum for PV/TE application. This method is the combination of anti-reflection and light-trapping for ultra-broadband photon management. The authors used crystalline silicon thin-film solar cells and nanostructures were used on the front and back side. Finite Difference Time Domain method was used for the numerical simulation. A new composite surface structure made up of moth-eye and inverted parabolic surface which could be used for anti-reflection in ultra-broadband wavelengths was proposed by the authors (Fig. 33). Results obtained showed that the use of anti-reflection and light-trapping method could improve the absorptivity of the solar cell while also improving the transmission of unused solar radiation to the thermoelectric generator. Therefore, the performance of the hybrid PV/TEG could be enhanced.

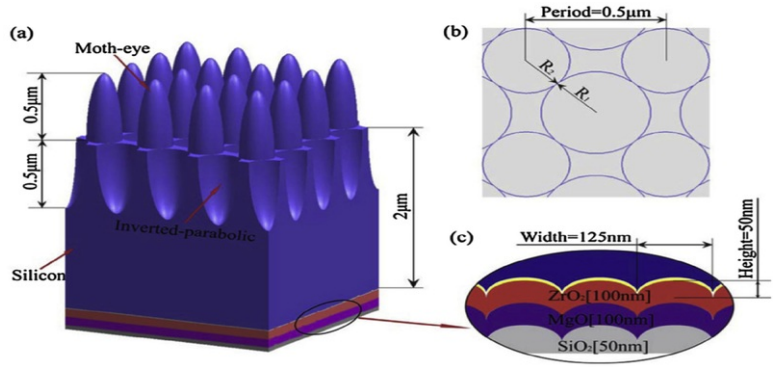

Fig. 33 (a) Silicon solar cell structure, (b) top view of solar cell structure and (c) cross-view of bottom antireflection coating [109]. (For interpretation of the references to colour in this figure legend, the reader is referred to the Web version of this article.)

alt-text: Fig. 33

Another research on advanced photon management for hybrid PV/TEG system was carried out by Zhang and Xuan [110]. The absorptance of photons with wavelengths of 0.3–11 μm capable of generating electron-hole pairs was enhanced by the use of biomimetic parabolic-shaped structure on the silicon film and a thin SiO_2 film at the bottom of the silicon film as the back-antireflection coating. Therefore, photons with wavelengths of 1.1–2.5 μm could pass through the structured surfaced and were absorbed by the TEG thus, the overall efficiency of the hybrid system was increased. Finally, the authors argued that the use of omnidirectional broadband photon management can enhance the performance of hybrid systems.

Zhang et al. [111] performed a feasibility study on the performance of a hybrid PV/TEG system employing perovskite solar cells. The influence of thermal concentration, solar selective absorber (SSA) and optical concentration ratio on the performance of the hybrid system was studied using three-dimensional numerical simulation. The advantage of using the perovskite solar cell is its large band gap and lower temperature coefficient. Results obtained showed that the temperature coefficient of the perovskite solar cell was lower than 0.02/K thus, the authors argued that the perovskite solar cell is a better choice for hybrid PV/TEG system compared to silicon solar and dye-sensitized solar cell. Recently, Xu et al. [112] presented an experimental study of a perovskite PV/TEG system. The TEG (Bi_2Te_3) was attached to the carbon side of the perovskite solar cell (PSC) using thermal silicon paste while the PSC was fabricated using the mesoscopic TiO_2/ZrO_2/carbon structure. Results obtained showed that the hybrid system achieved a maximum power

output of 20.3% and open circuit voltage of 1.29 V under 100 mW/cm^2 irradiance.

The use of solar cell and nanostructured thermoelectric material in hybrid PV/TEG system was investigated by Rabari et al. [113]. Nanostructured Bismuth Antinomy Telluride (BiSbTe) thermoelectric material was used and its power generation capability was compared with the traditional BiSbTe. Temperature dependent nanostructured thermoelectric material properties were considered and the influence of solar radiation and convective heat transfer coefficient on the hybrid system performance were studied. The authors argued that the nanostructured thermoelectric material enhanced the performance of the TEG.

5.7 Maximum power tracking and control system

One of the disadvantages of the hybrid PV/TEG system is the greater need for accurate maximum power point tracking (MPPT) system because the hybrid configuration results in a reduced fill factor value thus, the PV only system and the hybrid system have different maximum power point as shown in Fig. 34 [114]. In fact, Babu et al. [48] identified the need for effective MPPT algorithm as one of the research gaps in hybrid PV/TEG. Maximum power point tracking is simply an algorithm used in charge controllers for accurately determining the maximum available power from a PV or TEG under certain conditions. Voltage at which maximum power is produced is called maximum power point or peak power voltage. Factor such as solar radiation, ambient temperature and operating temperature influence the maximum power point.

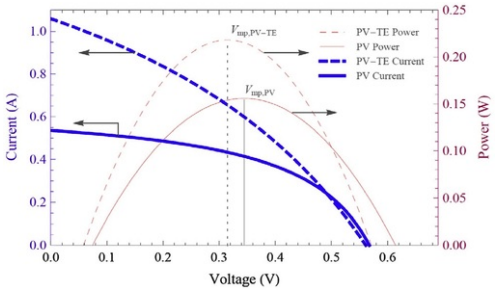

Fig. 34 PV/TEG and PV current-voltage characteristics [114].

alt-text: Fig. 34

Zhang et al. [115] presented a hybrid PV/TEG system with a MPPT control strategy which enabled the maximum power output of the PV and TEG to be obtained simultaneously. The developed system could be used in hybrid electric vehicles and an experimental validation of the proposed system was done. The developed system consisted of PV, TEG, power conditioning circuit, digital signal processor (DSP) controller and a battery serving as the load. The power conditioning circuit was used to track the maximum power point of the hybrid system by tuning the duty cycle of the pulse width modulator (PWM) switching signal to ensure the input resistance was equal to the internal resistance of the hybrid system. In this study, the single-ended primary-inductor converter (SEPIC) circuit was used.

An improved research [116] was carried out by the same authors in Ref. [115] using a similar approach. The hybrid PV/TEG system (Fig. 35) was developed for use in automobiles and a power conditioning circuit using MPPT was developed for enhanced hybrid system power output. Ćuk–Ćuk multiple input convert (MIC) was implemented on the hybrid system because it could offer non-pulsating input and output currents which could reduce the level of disturbance on the system operation significantly thus, increasing the battery life span. The authors stated that the difference between the Ćuk–Ćuk MIC and the SEPIC-SEPIC MIC is that the former needs only three inductors while the later needs four inductors thus, Ćuk–Ćuk MIC offers a lower cost, lighter weight and smaller volume. Results obtained showed that the overall hybrid system power output was enhanced by the Ćuk–Ćuk MIC using the MPPT.

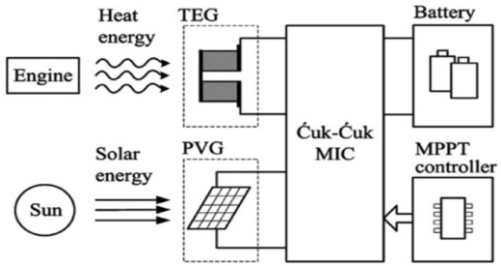

Fig. 35 Hybrid PV/TEG system with the Ćuk–Ćuk MIC [116].

alt-text: Fig. 35

Adopting a similar approach to Ref. [116], Fathima et al. [117] presented the use of Ćuk converters to enhance the performance of hybrid PV/TEG system and reduce the system noise/disturbance. Pulse generator circuit were used in designing the MPPT system and a microcontroller was used to change the duty cycle of the Ćuk converter. Results obtained showed that the designed MPPT system using Ćuk converter could function in Boost, Buck-Boost or Buck mode therefore, the hybrid system power output could be enhanced.

Jung et al. [118] presented the use of a single-inductor, dual-input and dual-output boost convert with a novel time-multiplexing MPPT algorithm to enhance the performance of a hybrid PV/TEG system. The authors argued that the developed time-multiplexing MPPT algorithm enabled the boost converter to achieve MPPT for the hybrid system using a single clock frequency. Therefore, the hybrid system efficiency was increased, and the boost converted was designed using 65 nm complementary metal-oxide-semiconductor (CMOS) technology. Finally, a peak efficiency of 78% was obtained by the hybrid system.

Verma et al. [119] developed a dynamic model in MATLAB/Simulink environment to study the performance of a hybrid PV/TEG system (Fig. 36). The effectiveness of MPPT system under varying load and solar radiation was studied and it was found that the control scheme used in this study ensured optimum hybrid system values were obtained while preventing the PV and TEG from operating at temperatures above the prescribed limits. A DC-DC boost converter was used to ensure the effective of the MPPT system. In addition, the hybrid system was controlled using a master-slave configuration where the battery source operated as the Master for both the PV and TEG. Results obtained showed that the used master-slave configuration ensured the smooth operation of the hybrid system.

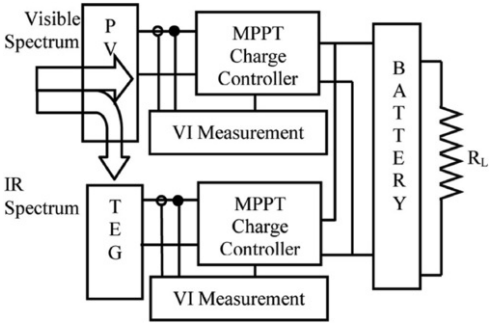

Fig. 36 Proposed hybrid system with MPPT for waste heat recovery [119].

alt-text: Fig. 36

Kwan and Wu [120] presented the application of Lock-On mechanism MPPT algorithm to hybrid PV/TEG systems. A detailed experimental and numerical investigation was carried out on the capability of Lock-On Mechanism (LOM) algorithm to achieve maximum power point tracking for hybrid PV/TEG system. The LOM algorithm was applied to a double SEPIC converter and the numerical simulation was performed using the MATLAB/Simulink environment (Fig. 37). The double SEPIC converter used was made up of two single SEPIC converters and their output capacitors were connected in parallel together. Results obtained from the experimental and numerical investigation carried out showed that the Lock-On Mechanism MPPT algorithm performs better than the conventional hill climbing algorithm.

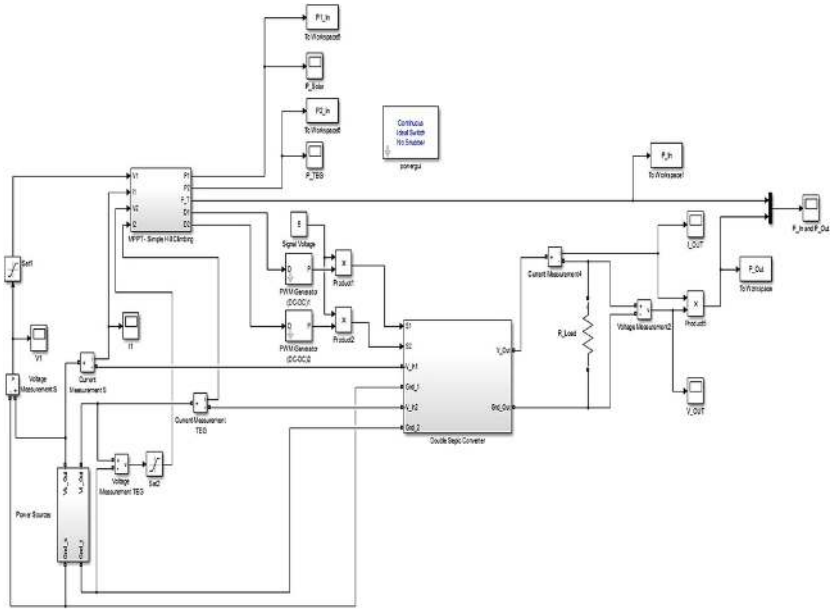

Fig. 37 Hybrid system with MPPT Simulink model using hill climbing algorithm [120].

alt-text: Fig. 37

5.8 Niche applications

Yu et al. [121] investigated a PV/TEG for powering wireless sensor networks. The developed system consisted of a PV, TEG and heat sink with air cooling. Compared to a single PV, the PV in the hybrid system had an efficiency increase of 5.2% due to a solar cell temperature reduction of 13 °C. Energy storage devices were incorporated into the hybrid system to store energy for use during periods of low solar irradiance. A lithium ion battery with storage capacity of 1400 mAh and an ultra-capacitor with storage capacity of 30 F were used to store energy from the PV and TEG respectively. The developed hybrid system had the capacity to renew energy by itself thus it could provide reliable and long-time power to the sensor node.

Leonov et al. [122] investigated the use of a PV/TEG to power an autonomous medical device: electroencephalography (EEG) in a shirt. The device was battery free and the PV was positioned about the radiators used to heat up the TEG (Fig. 38). The authors developed an ultralow power biopotential readout integrated circuit which had a power consumption of 60 μW per channel. The signal quality provided by the readout was the same with that of modern ambulatory systems and the developed system had an extra advantage of being wireless compared to wired commercial systems thus, the biopotential signals could be transmitted to a doctor in real time.

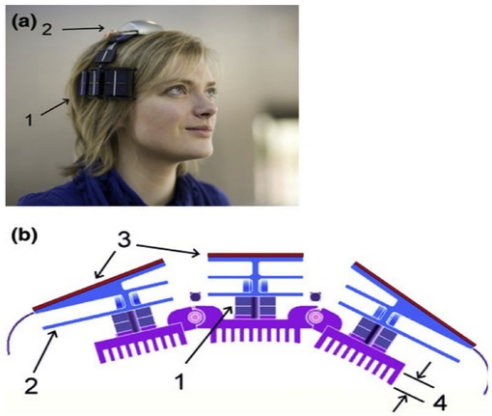

Fig. 38 (a) Electroencephalography diadem: (1) right-side hybrid module, and (2) electronic module and 2.4 GHz wireless link. (b) Schematic cross-section of hybrid module: (1) thermophile, (2) radiator, (3) PV cells, and (4) thermal shunts [122].

alt-text: Fig. 38

The feasibility of PV/TEG for terrestrial and space applications was investigated by Da et al. [123]. A similar approach used by Ref. [109] was employed in this study which is the use of photon and thermal management to enhance the performance of the hybrid PV/TEG system. The authors used bio-inspired moth-eye nanostructured surface to suppress the full solar spectrum photons reflection and an enhanced transmission film was used to improve the system performance. Results obtained showed that for hybrid PV/TEG systems, low concentration ratio is better especially when used in terrestrial and space applications. In addition, the results showed that the hybrid system without optical concentration performed better than the PV only system. It was also found that for terrestrial application (corresponding to Air Mass 1.5), the overall hybrid system efficiency increased from 13.79 to 18.51% due to the use of the moth-eye structured surface. While for space application (Air Mass 0), the use of the moth-eye structured in the hybrid system increased the efficiency to 16.84% (Fig. 39).

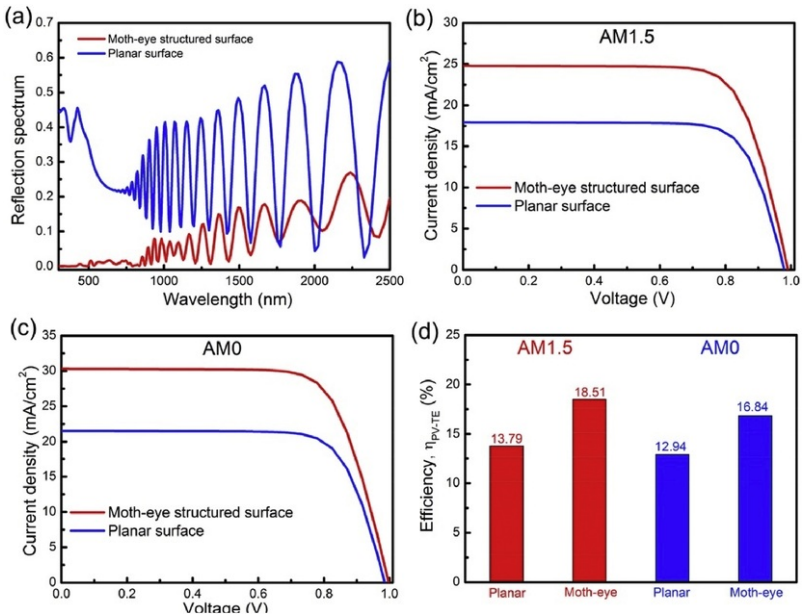

Fig. 39 Performance comparison between moth-eye structured surface and planar surface. (a) Reflection spectrum, (b) solar cell characteristics under AM 1.5, (c) solar cell characteristics under AM 0 and (d) hybrid system efficiency [123].

alt-text: Fig. 39

Kwan et al. [124] studied the performance of a hybrid PV/TEG system for outer space application. A multi-objective Non-dominated Sorting Genetic Algorithm (NSGA-II) was used to optimize the thermoelectric generator design for obtaining maximum power output. In addition, the authors compared the performance of a single stage and two stage thermoelectric generator. Results obtained from this study showed that for space applications, the power generation contribution of the thermoelectric generator in a hybrid PV/TEG system is negligible. Furthermore, it was observed that single stage TEG is for hybrid PV/TEG systems compared to two stage TEG. Finally, the authors also argued that the optimized PV/TEG system had a lower efficiency compared to the PV only system. This finding is in agreement with other similar findings like [83,84].

Considering the actual weather conditions of three different sample cities in Europe, Rezania et al. [125] developed a model to predict the performance of hybrid PV/TEG system under such conditions. The influence of solar irradiation, wind speed, ambient temperature, convective and radiated heat losses were all accounted for in the model. It was found that radiated heat loss on the surface of the PV and convective heat loss due to wind speed are the most important parameters influencing the hybrid system performance. Comparing the performance of the hybrid system in the sample locations, it was found that maximum power output was obtained during spring period in Northern Europe while for Southern Europe, the maximum power output was obtained during summer period.

Ariffin et al. [126] presented a conceptual design of a hybrid PV/TEG system for application in an automated greenhouse system project (Fig. 40). The developed system was compared to conventional PV only system and the authors provided recommendations for future works. They recommended the use of automated semi-transparent thin film solar panel to efficiently absorb solar radiations. An experimental and numerical investigation was carried out and the effectiveness of using hybrid PV/TEG in an automated greenhouse system was demonstrated.

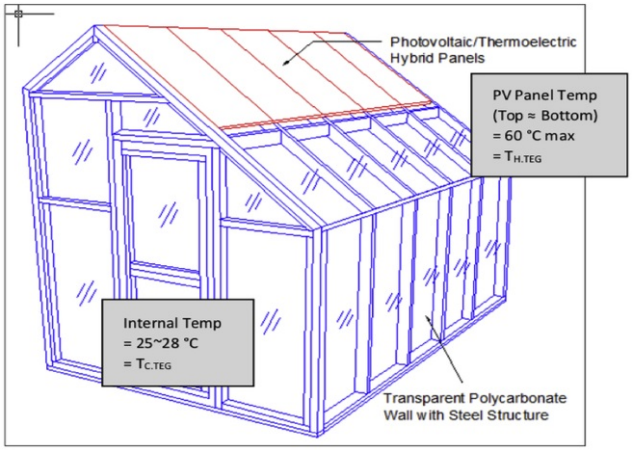

Fig. 40 Conceptual design of a hybrid PV/TEG for automated greenhouse system [126].

alt-text: Fig. 40

6 Discussion and recommendations

Passive cooling of photovoltaic-thermoelectric generator is an interesting research area being explored due to the effectiveness of passive cooling devices like heat pipe in significantly reducing the temperature of photovoltaic cells. Heat pipes are efficient heat transfer devices that can transport heat over a long distance with small temperature gradient [127]. Therefore, the use of heat pipes in a hybrid PV/TEG system could reduce the quantity of TEG used in the thermal management of photovoltaic cells while also providing an enhanced overall performance [128]. Flat plate microchannel heat pipes are more efficient than cylindrical heat pipe because of the reduced thermal contact resistance between the surface of the PV and heat pipe due to the shape of the heat pipe. Therefore, more research on the integration of hybrid PV/TEG with flat plate microchannel heat pipes are strongly recommended especially because of the encouraging results reported from such heat pipe hybrid systems by Refs. [127,128].

Several researchers [9,58,59,91] have agreed that the performance of a thermoelectric generator in a hybrid system can be enhanced by material and structural optimization. A lot of material optimization efforts are being carried out on improving the efficiency of the PV and TE. Some of this research have obtained significant results as presented in Section 5.6. Improving the thermoelectric figure of merit is the major research task for increasing the efficiency of the TE. A 50% increase in hybrid system efficiency could be achieved simply by using TEG with higher figure of merit compared to the currently available ones [55]. The use of nanostructured materials has also been gaining momentum recently due to the good results obtained thus, more research is encouraged on hybrid PV/TEG systems with nanostructure materials. In addition, more research is encouraged in the area of PV surface absorptivity. Increasing the absorptivity of PV could significantly increase its efficiency thus, more research on photon management of hybrid PV/TEG is highly recommended. Furthermore, the optimization of the TE structure is necessary to enhance the performance of the hybrid system. Efforts made on the structural/geometry optimization of the TE have been presented in Section 5.3. In spite of the plethora of research available on TEG optimization, its integration with PV necessitates new investigations be made due to the complex relationship between the PV and TEG. While one requires more temperature for higher performance (TEG), the other system (PV) prefers the opposite. Thus, more research on the efficient coupling of PV/TEG is needed especially considering the thermal contact resistance in the hybrid system. In addition, a lossless coupling would be very good for the hybrid system performance and it is very important to remember that results obtained from TEG only optimization is not sufficient for the hybrid system optimization. Therefore, the optimized load resistance and geometry of the TEG in a TEG only system is different from the one in a hybrid system due to the influence of the PV.

Only a few research has been conducted on spectrum splitting PV/TEG (Table 4) however, sufficient works have been done on direct coupling PV/TEG system (Table 5). It is therefore recommended that more attention be paid to spectrum splitting hybrid systems due to their potentially high performance when properly optimized. Furthermore, Cooling is an integral part of any TEG system as its directly affects the system performance significantly. Therefore, the hybrid PV/TEG system needs efficient cooling systems capable of creating a larger temperature difference across the TE while also reducing the temperature of the PV. From the detailed review carried out in Section 5.4, the consensus is that water cooling is more effective than air cooling. However, the introduction of nanofluid cooling into hybrid PV/TEG systems has resulted in significantly lower temperature on the TEG cold side compared to water cooling therefore, more research on PV/TEG using nanofluid is suggested. However, the extra cost of nanofluid must be taken into consideration and a justification must be made in terms of overall performance compared to hybrid systems with cheap conventional cooling.

Due to the intermittent nature of solar energy, storage systems have been incorporated into the hybrid PV/TEG to store energy for use during periods of low irradiance. The use of phase change material (PCM) seems to be the best option due to its unique capability to store a significant amount of heat and thus mitigate the temperature fluctuations in the hybrid system. More research on the hybrid systems with PCM is suggested however, again the extra cost must be considered. A limiting factor to the enhancement of hybrid system performance is the need for opportunity cost analysis. While there are obvious ways to easily improve the performance of the system, a trade-off must be made due to the high cost of such optimization.

The use of concentrated solar energy is an easy way to improve the hybrid system efficiency however, care must be taken not to damage the PV by over applying high concentration. It is widely known that the performance of the PV reduces with temperature

however, when high concentration is properly applied, the overall performance of the system could be increased. Thus, there is a need to properly determine the concentration ratio for optimized performance. Some research has been conducted using the concept of changing the position of the concentrator in the hybrid system. Rather than applying the high concentration on the PV surface traditionally, it is applied to the TE surface instead. This way, the PV can operate at a low temperature while the TE can operate at a high temperature. Notwithstanding, this technique seems to place emphasis on the use of TEG for additional energy generation however, it is widely known that the PV contributes more to the overall hybrid system performance (power output and efficiency) thus, it might be worth considering placing more emphasis on optimizing the PV for high performance by using the TEG more has a cooling device than a power generator. The TEG is an effective waste heat recovery device thus, reducing the temperature of the PV should be the focus of hybrid PV/TEG system optimization.

A profusion of literature exists on the steady state performance of hybrid PV/TEG systems however, the actual performance of the hybrid system is affected by the daily variations in weather condition. Thus, more research is needed on the hybrid system performance under transient conditions. In addition, very few research works on hybrid PV/TEG systems have been conducted with the use of finite element method (FEM). Contrarily, there is an abundance of research on the one-dimensional simulation using MATLAB/Simulink. The advantage of using FEM is that, it can be used for three-dimensional study of the actual system. Thus, it provides more realistic results and better optimization efforts can be made using this method. Finite element method has Multiphysics capability thus it is highly suggested for deep research on hybrid PV/TEG. In addition, FEM allows the Thomson effects and temperature dependent thermoelectric properties to be easily coupled and it provides a user-friendly interface for easily visualization of results [91].

More research on thermophotovoltaic/thermoelectric (TPV/TE) systems is recommended due to its unique advantages. Thermophotovoltaic (TPV) cells are capable of converting infrared radiation thus, when thermal emitter are used as the source for TPV systems, they can operate all day as they wouldn't be affected by the intermittent nature of the solar energy [129]. Recently, a first of its kind study on hybrid TPV/TE was conducted by Ref. [130]. Results obtained showed that the TPV/TE system performed better than the TE and TPV only systems. More research on such systems is highly recommended as an alternative to the conventional hybrid PV/TEG systems. Furthermore, more research on the combination of TEG, TEC and PV is recommended due to the encouraging results obtained by Refs. [131,132]. The basic idea is to combine the advantages of each individual systems and obtain a better performing hybrid system. In such systems, the thermoelectric cooler is used to cool the PV while the TEG is used as the heat sink for the TEC, thus the overall performance of the hybrid system is increased, and additional energy is generated. However, more research needs to be conducted on the feasibility of such systems as it could potentially provide a better performance compared to the hybrid PV/TEG systems.

7 Conclusion

Owing to the fast rate at which the field of PV/TEG is growing and the numerous significant research being carried, this review was written to present and discuss the state of art in the field of PV/TEG. Thermoelectric generators offer unique advantages which when combined with the photovoltaic can result in an enhanced hybrid system performance and wider utilization of the solar spectrum. PV/TEG offers an alternative to the very well researched and widely used PV/T systems. The same idea is used in both systems which is to enhance the performance of the PV by reducing its temperature and producing additional energy. This review presented a detailed overview of all research areas and optimization efforts relating to hybrid PV/TEG. The use of concentrated solar energy for hybrid PV/TEG was discussed, key focus areas in the hybrid system research such as: TEG geometry optimization, Energy storage, TEG cooling, PV and TE material optimization were all discussed in detail. Niche application of PV/TEG were also presented to show its wide applicability in various fields and not just electricity generation. The significance of maximum power point tracking in hybrid PV/TEG was also discussed and a summary of the most recently published works in hybrid PV/TEG was presented. Finally, a deep discussion of all the results obtained from the extension literatures reviewed was presented and more importantly, recommendations for future works were provided. A thorough investigation of hybrid PV/TEG systems has been performed in this research and it is envisaged that this review would serve as an indispensable literature on hybrid PV/TEG.

Acknowledgement

This study was sponsored by the Project of EU Marie Curie International incoming Fellowships Program (745614). The authors would also like to express our appreciation for the financial supports from EPSRC (EP/R004684/1) and Innovate UK (TSB 70507-481546) for the Newton Fund - China-UK Research and Innovation Bridges Competition 2015 Project ‘A High Efficiency, Low Cost and Building Integrate-able Solar Photovoltaic/Thermal (PV/T) system for Space Heating, Hot Water and Power Supply’ and DongGuan Innovation Research Team Program (No. 2014607101008).

References

[1] R.K. Akikur, R. Saidur, H.W. Ping and K.R. Ullah, Comparative study of stand-alone and hybrid solar energy systems suitable for off-grid rural electrification: a review, *Renew Sustain Energy Rev* **27**, 2013, 738–752, https://doi.org/10.1016/j.rser.2013.06.043.

[2] M.A. Al-Nimr, B.M. Tashtoush, M.A. Khasawneh and I. Al-Keyyam, A hybrid concentrated solar thermal collector/thermo-electric generation system, *Energy* **134**, 2017, 1001–1012, https://doi.org/10.1016/j.energy.2017.06.093.

[3] M. Thirugnanasambandam, A. Review of solar thermal technologies, *Renew Sustain Energy Rev* **14**, 2010, 312–322, https://doi.org/10.1016/j.rser.2009.07.014.

[4] N. Dimri, A. Tiwari and G.N. Tiwari, Thermal modelling of semitransparent photovoltaic thermal (PVT) with thermoelectric cooler (TEC) collector, *Energy Convers Manag* **146**, 2017, 68–77, https://doi.org/10.1016/j.enconman.2017.05.017.

[5] A. Makki, S. Omer and H. Sabir, Advancements in hybrid photovoltaic systems for enhanced solar cells performance, *Renew Sustain Energy Rev* **41**, 2015, 658–684, https://doi.org/10.1016/j.rser.2014.08.069.

[6] F. Grubisić-Čabo, S. Nizetić and T.G. Marco, Photovoltaic panels: a review of the cooling techniques, *Trans FAMENA* **40**, 2016, 63–74, https://doi.org/10.1017/S0020818300000849.

[7] W. He, G. Zhang, X. Zhang, J. Ji, G. Li and X. Zhao, Recent development and application of thermoelectric generator and cooler, *Appl Energy* **143**, 2015, 1–25 https://doi.org/10.1016/j.apenergy.2014.12.075.

[8] G. Li, S. Shittu, T.M.O. Diallo, M. Yu, X. Zhao and J. Ji, A review of solar photovoltaic-thermoelectric hybrid system for electricity generation, *Energy* **158**, 2018, 41–58, https://doi.org/10.1016/j.energy.2018.06.021.

[9] S. Shittu, G. Li, X. Zhao, X. Ma, Y.G. Akhlaghi and E. Ayodele, High performance and thermal stress analysis of a segmented annular thermoelectric generator, *Energy Convers Manag* **184**, 2019, 180–193, https://doi.org/10.1016/j.enconman.2019.01.064

[10] G. Li, W. Feng, Y. Jin, X. Chen and J. Ji, Discussion on the solar concentrating thermoelectric generation using micro-channel heat pipe array, *Heat Mass Transf* **53**, 2017, 3249–3256, https://doi.org/10.1007/s00231-017-2026-3.

[11] D. Narducci, P. Bermel, B. Lorenzi and N. Wang, Hybrid and fully thermoelectric solar harvesting, first ed., 2018, Springer International Publishing; Switzerland, https://doi.org/10.1109/IPDPS.2006.1639640.

[12] D.M. Chapin, C.S. Fuller and G.L. Pearson, A new silicon p-n junction photocell for converting solar radiation into electrical power [3], *J Appl Phys* **25**, 1954, 676–677, https://doi.org/10.1063/1.1721711.

[13] L. El Chaar, L.A. Lamont and N. El Zein, Review of photovoltaic technologies, *Renew Sustain Energy Rev* **15**, 2011, 2165–2175, https://doi.org/10.1016/j.rser.2011.01.004.

[14] P.G.V. Sampaio, M.O.A. González, R.M. de Vasconcelos, M.A.T. dos Santos, J.C. de Toledo and J.P.P. Pereira, Photovoltaic technologies: mapping from patent analysis, *Renew Sustain Energy Rev* **93**, 2018, 215–224, https://doi.org/10.1016/j.rser.2018.05.033.

[15] P. Huen and W.A. Daoud, Advances in hybrid solar photovoltaic and thermoelectric generators, *Renew Sustain Energy Rev* **72**, 2017, 1295–1302, https://doi.org/10.1016/j.rser.2016.10.042.

[16] M.A. Green, Y. Hishikawa, E.D. Dunlop, D.H. Levi, J. Hohl-Ebinger and A.W.Y. Ho-Baillie, Solar cell efficiency tables (version 52), *Prog Photovoltaics Res Appl* **26**, 2018, 427–436, https://doi.org/10.1002/pip.3040.

[17] P. Singh, S.N. Singh, M. Lal and M. Husain, Temperature dependence of I-V characteristics and performance parameters of silicon solar cell, *Sol Energy Mater Sol Cells* **92**, 2008, 1611–1616, https://doi.org/10.1016/j.solmat.2008.07.010.

[18] M. Fisac, F.X. Villasevil and A.M. López, High-efficiency photovoltaic technology including thermoelectric generation, *J Power Sources* **252**, 2014, 264–269, https://doi.org/10.1016/j.jpowsour.2013.11.121.

[19] O. Dupré, R. Vaillon and M.A. Green, Thermal behavior of photovoltaic devices, 2017, Springer International Publishinghttps://doi.org/10.1007/978-3-319-49457-9.

[20] X. Zhang, X. Zhao, S. Smith, J. Xu and X. Yu, Review of R & D progress and practical application of the solar photovoltaic/thermal (PV/T) technologies, *Renew Sustain Energy Rev* **16**, 2012, 599–617, https://doi.org/10.1016/j.rser.2011.08.026.

[21] J.F. Li, W.S. Liu, L.D. Zhao and M. Zhou, High-performance nanostructured thermoelectric materials, *NPG Asia Mater* **2**, 2010, 152–158, https://doi.org/10.1038/asiamat.2010.138.

[22] D.M. Rowe, Thermoelectric handbook: macro to nano, 2006, CRC Press, Taylor & Francis Group.

[23] A.J. Minnich, M.S. Dresselhaus, Z.F. Ren and G. Chen, Bulk nanostructured thermoelectric materials: current research and future prospects, *Energy Environ Sci* **2**, 2009, 466–479, https://doi.org/10.1039/b822664b.

[24] M.H. Elsheikh, D.A. Shnawah, M.F.M. Sabri, S.B.M. Said, H.M. Hassan, A.M.B. Bashir, et al., A review on thermoelectric renewable energy: principle parameters that affect their performance, *Renew Sustain Energy Rev* **30**, 2014, 337–355, https://doi.org/10.1016/j.rser.2013.10.027.

[25] S.B. Riffat and X. Ma, Improving the coefficient of performance of thermoelectric cooling systems: a review, *Int J Energy Res* **28**, 2004, 753–768, https://doi.org/10.1002/er.991.

[26] M. Martín-González, O. Caballero-Calero and P. Díaz-Chao, Nanoengineering thermoelectrics for 21st century: energy harvesting and other trends in the field, *Renew Sustain Energy Rev* **24**, 2013, 288–305, https://doi.org/10.1016/j.rser.2013.03.008.

[27] A.R.M. Siddique, S. Mahmud and B. Van Heyst, A review of the state of the science on wearable thermoelectric power generators (TEGs) and their existing challenges, *Renew Sustain Energy Rev* **73**, 2017, 730–744, https://doi.org/10.1016/j.rser.2017.01.177.

[28] X.F. Zheng, C.X. Liu, Y.Y. Yan and Q. Wang, A review of thermoelectrics research - recent developments and potentials for sustainable and renewable energy applications, *Renew Sustain Energy Rev* **32**, 2014, 486–503, https://doi.org/10.1016/j.rser.2013.12.053.

[29] S. Twaha, J. Zhu, Y. Yan and B. Li, A comprehensive review of thermoelectric technology: materials, applications, modelling and performance improvement, *Renew Sustain Energy Rev* **65**, 2016, 698–726, https://doi.org/10.1016/j.rser.2016.07.034.

[30] J. Yang, Potential applications of thermoelectric waste heat recovery in the automotive industry, In: *Int conf thermoelectr ICT, proc 2005,* 2005, 155–159, https://doi.org/10.1109/ICT.2005.1519911.

[31] K.M. Saqr, M.K. Mansour and M.N. Musa, Patient expectations for health supervision advice in continuity clinic: experience from a teaching hospital in Thailand, *Int J Automot Technol* **9**, 2008, 155–160, https://doi.org/10.1007/s12239.

[32] Y.Y. Hsiao, W.C. Chang and S.L. Chen, A mathematic model of thermoelectric module with applications on waste heat recovery from automobile engine, *Energy* **35**, 2010, 1447–1454, https://doi.org/10.1016/j.energy.2009.11.030.

[33] G. Shu, X. Ma, H. Tian, H. Yang, T. Chen and X. Li, Configuration optimization of the segmented modules in an exhaust-based thermoelectric generator for engine waste heat recovery, *Energy* **160**, 2018, 612–624, https://doi.org/10.1016/j.energy.2018.06.175.

[34] L. Francioso, C. De Pascali, I. Farella, C. Martucci, P. Cretì, P. Siciliano, et al., Flexible thermoelectric generator for wearable biometric sensors, *Proc IEEE Sensors* **196**, 2010, 747–750, https://doi.org/10.1109/ICSENS.2010.5690757.

[35] S.J. Kim, J.H. We and B.J. Cho, A wearable thermoelectric generator fabricated on a glass fabric, *Energy Environ Sci* **7**, 2014, 1959–1965, https://doi.org/10.1039/c4ee00242c.

[36] F. Suarez, D.P. Parekh, C. Ladd, D. Vashaee, M.D. Dickey and M.C. Öztürk, Flexible thermoelectric generator using bulk legs and liquid metal interconnects for wearable electronics, *Appl Energy* **202**, 2017, 736–745, https://doi.org/10.1016/j.apenergy.2017.05.181.

[37] S. Qing, A. Rezania, L.A. Rosendahl and X. Gou, Design of flexible thermoelectric generator as human body sensor, *Mater Today Proc* **5**, 2018, 10338–10346, https://doi.org/10.1016/j.matpr.2017.12.282.

[38] R. Amatya and R.J. Ram, Solar thermoelectric generator for micropower applications, *J Electron Mater* **39**, 2010, 1735–1740, https://doi.org/10.1007/s11664-010-1190-8.

[39] D. Madan, Z. Wang, P.K. Wright and J.W. Evans, Printed flexible thermoelectric generators for use on low levels of waste heat, *Appl Energy* **156**, 2015, 587–592, https://doi.org/10.1016/j.apenergy.2015.07.066.

[40] P. Pichanusakorn and P. Bandaru, Nanostructured thermoelectrics, *Mater Sci Eng R Rep* **67**, 2010, 19–63, https://doi.org/10.1016/j.mser.2009.10.001.

[41] S.B. Riffat and X. Ma, Thermoelectrics: a review of present and potential applications, *Appl Therm Eng* **23**, 2003, 913–935, https://doi.org/10.1016/S1359-4311(03)00012-7.

[42] G. Moore and W. Peterson, Solar PV-thermoelectric generator hybrid system: case studies, In: *10th int. Telecommun. Energy conf., san diego, California, USA,* 1988, 308–311.

[43] G. Contento, B. Lorenzi, A. Rizzo and D. Narducci, Efficiency enhancement of a-Si and CZTS solar cells using different thermoelectric hybridization strategies, *Energy* **131**, 2017, 230–238, https://doi.org/10.1016/j.energy.2017.05.028.

[44] B. Lorenzi, M. Acciarri and D. Narducci, Experimental determination of power losses and heat generation in solar cells for photovoltaic-thermal applications, *J Mater Eng Perform* **27**, 2018, 6291–6298, https://doi.org/10.1007/s11665-018-3604-3.

[45] J.R. Howell, R. Siegel and M.P. Mengüç, Thermal radiation heat transfer, fifth ed., 2010, CRC Press, Taylor & Francis Group; New York.

[46] T.M. Tritt, H. Böttner and L. Chen, Thermoelectrics : direct solar thermal energy conversion, *Harnessing Mater Energy* **33**, 2008, 366–368, https://doi.org/10.1016/0038-092X(80)90311-4.

[47] B. Lorenzi, G. Contento, V. Sabatelli, A. Rizzo and D. Narducci, Theoretical analysis of two novel hybrid thermoelectric-photovoltaic systems based on, *J Nanosci Nanotechnol* **17**, 2017, 1608–1615, https://doi.org/10.1166/jnn.2017.13722.

[48] C. Babu and P. Ponnambalam, The role of thermoelectric generators in the hybrid PV/T systems: a review, *Energy Convers Manag* **151**, 2017, 368–385, https://doi.org/10.1016/j.enconman.2017.08.060.

[49] D. Kraemer, L. Hu, A. Muto, X. Chen, G. Chen and M. Chiesa, Photovoltaic-thermoelectric hybrid systems: a general optimization methodology, *Appl Phys Lett* **92**, 2008, 243503, https://doi.org/10.1063/1.2947591.

[50] X. Ju, Z. Wang, G. Flamant, P. Li and W. Zhao, Numerical analysis and optimization of a spectrum splitting concentration photovoltaic-thermoelectric hybrid system, *Sol Energy* **86**, 2012, 1941–1954, https://doi.org/10.1016/j.solener.2012.02.024.

[51] E. Yin, Q. Li and Y. Xuan, A novel optimal design method for concentration spectrum splitting photovoltaicethermoelectric hybrid system, *Energy* **163**, 2018, 519–532, https://doi.org/10.1016/j.apenergy.2018.05.127.

[52] Z. Yang, W. Li, X. Chen, S. Su, G. Lin and J. Chen, Maximum efficiency and parametric optimum selection of a concentrated solar spectrum splitting photovoltaic cell-thermoelectric generator system, *Energy Convers Manag* **174**, 2018, 65–71, https://doi.org/10.1016/j.enconman.2018.08.038.

[53] R. Bjørk and K.K. Nielsen, The maximum theoretical performance of unconcentrated solar photovoltaic and thermoelectric generator systems, *Energy Convers Manag* **156**, 2018, 264–268, https://doi.org/10.1016/j.enconman.2017.11.009.

[54] D. Liang, Q. Luo, P. Li, Y. Fu, L. Cai and P. Zhai, Optimization and experimentation of concentrating photovoltaic/cascaded thermoelectric generators hybrid system using spectral beam splitting technology, *IOP Conf Ser Earth Environ Sci* **199**, 2018, , 052044https://doi.org/10.1088/1755-1315/199/5/052044.

[55] W.G.J.H.M. Van Sark, Feasibility of photovoltaic - thermoelectric hybrid modules, *Appl Energy* **88**, 2011, 2785–2790, https://doi.org/10.1016/j.apenergy.2011.02.008.

[56] E. Yin, Q. Li and Y. Xuan, One-day performance evaluation of photovoltaic-thermoelectric hybrid system, *Energy* **143**, 2018, 337–346, https://doi.org/10.1016/j.energy.2017.11.011.

[57] E. Yin, Q. Li and Y. Xuan, Optimal design method for concentrating photovoltaic-thermoelectric hybrid system, *Appl Energy* **226**, 2018, 320–329, https://doi.org/10.1016/j.apenergy.2018.05.127.

[58] G. Li, S. Shittu, X. Ma and X. Zhao, Comparative analysis of thermoelectric elements optimum geometry between Photovoltaic-thermoelectric and solar thermoelectric, *Energy* **171**, 2019, 599–610, https://doi.org/10.1016/j.energy.2019.01.057.

[59] S. Mahmoudinezhad, S.A. Atouei, P.A. Cotfas, D.T. Cotfas, L.A. Rosendahl and A. Rezania, Experimental and numerical study on the transient behavior of multi- junction solar cell-thermoelectric generator hybrid system, *Energy Convers Manag* **184**, 2019 448–455, https://doi.org/10.1016/j.enconman.2019.01.081.

[60] E. Yin, Q. Li, D. Li and Y. Xuan, Experimental investigation on effects of thermal resistances on a photovoltaic-thermoelectric system integrated with phase change materials, *Energy* **169**, 2019, 172–185, https://doi.org/10.1016/j.energy.2018.12.035.

[61] A. Lekbir, M. Meddad, A. E, S. Benhadouga and R. Khenfer, Higher-efficiency for combined photovoltaic-thermoelectric solar power generation, *Int J Green Energy* **00**, 2019, 1–7, https://doi.org/10.1080/15435075.2019.1567515.

[62] O.F. Marandi, M. Ameri and B. Adelshahian, The experimental investigation of a hybrid photovoltaic-thermoelectric power generator solar cavity-receiver, *Sol Energy* **161**, 2018, 38–46, https://doi.org/10.1016/j.solener.2017.12.039.

[63] J. Zhang and Y. Xuan, An integrated design of the photovoltaic-thermoelectric hybrid system, *Sol Energy* **177**, 2019, 293–298, https://doi.org/10.1016/j.solener.2018.11.012.

[64] P.M. Rodrigo, A. Valera, E.F. Fernández and F.M. Almonacid, Performance and economic limits of passively cooled hybrid thermoelectric generator-concentrator photovoltaic modules, *Appl Energy* **238**, 2019, 1150–1162, https://doi.org/10.1016/J.APENERGY.2019.01.132.

[65] H.K. Lakeh, H. Kaatuzian and R. Hosseini, A parametrical study on photo-electro-thermal performance of an integrated thermoelectric-photovoltaic cell, *Renew Energy* **138**, 2019, 542–550, https://doi.org/10.1016/J.RENENE.2019.01.094.

[66] A. Lekbir, S. Hassani, M.R. Ab Ghani, C.K. Gan, S. Mekhilef and R. Saidur, Improved energy conversion performance of a novel design of concentrated photovoltaic system combined with thermoelectric generator with advance cooling system, *Energy Convers Manag* **177**, 2018, 19–29, https://doi.org/10.1016/j.enconman.2018.09.053.

[67] B. Lorenzi and G. Chen, Theoretical efficiency of hybrid solar thermoelectric-photovoltaic generators, *J Appl Phys* **124**, 2018, https://doi.org/10.1063/1.5022569.

[68] C. Babu and P. Ponnambalam, The theoretical performance evaluation of hybrid PV-TEG system, *Energy Convers Manag* **173**, 2018, 450–460, https://doi.org/10.1016/j.enconman.2018.07.104.

[69] P. Motiei, M. Yaghoubi, E. GoshtashbiRad and A. Vadiee, Two-dimensional unsteady state performance analysis of a hybrid photovoltaic-thermoelectric generator, *Renew Energy* **119**, 2018, 551–565, https://doi.org/10.1016/j.renene.2017.11.092.

[70] S. Mahmoudinezhad, A. Rezania and L.A. Rosendahl, Behavior of hybrid concentrated photovoltaic-thermoelectric generator under variable solar radiation, *Energy Convers Manag* **164**, 2018, 443–452, https://doi.org/10.1016/j.enconman.2018.03.025.

[71] H.R. Fallah Kohan, F. Lotfipour and M. Eslami, Numerical simulation of a photovoltaic thermoelectric hybrid power generation system, *Sol Energy* **174**, 2018, 537–548, https://doi.org/10.1016/j.solener.2018.09.046.

[72] Y.P. Zhou, M.J. Li, W.W. Yang and Y.L. He, The effect of the full-spectrum characteristics of nanostructure on the PV-TE hybrid system performances within multi-physics coupling process, *Appl Energy* **213**, 2018, 169–178, https://doi.org/10.1016/j.apenergy.2018.01.027.

[73] Y. Vorobiev, J. González-Hernández, P. Vorobiev and L. Bulat, Thermal-photovoltaic solar hybrid system for efficient solar energy conversion, *Sol Energy* **80**, 2006, 170–176, https://doi.org/10.1016/j.solener.2005.04.022.

[74] W. Zhu, Y. Deng, Y. Wang, S. Shen and R. Gulfam, High-performance photovoltaic-thermoelectric hybrid power generation system with optimized thermal management, *Energy* **100**, 2016, 91–101, https://doi.org/10.1016/j.energy.2016.01.055.

[75] R. Lamba and S.C. Kaushik, Modeling and performance analysis of a concentrated photovoltaic-thermoelectric hybrid power generation system, *Energy Convers Manag* **115**, 2016, 288–298, https://doi.org/10.1016/j.enconman.2016.02.061.

[76] R. Lamba and S.C. Kaushik, Solar driven concentrated photovoltaic-thermoelectric hybrid system: numerical analysis and optimization, *Energy Convers Manag* **170**, 2018, 34–49, https://doi.org/10.1016/j.enconman.2018.05.048.

[77] A. Rezania and L.A. Rosendahl, Feasibility and parametric evaluation of hybrid concentrated photovoltaic-thermoelectric system, *Appl Energy* **187**, 2017, 380–389, https://doi.org/10.1016/j.apenergy.2016.11.064.

[78] S. Mahmoudinezhad, A. Rezania, D.T. Cotfas, P.A. Cotfas and L.A. Rosendahl, Experimental and numerical investigation of hybrid concentrated photovoltaic – thermoelectric module under low solar concentration, *Energy* **159**, 2018, 1123–1131, https://doi.org/10.1016/j.energy.2018.06.181.

[79] K.T. Park, S.M. Shin, A.S. Tazebay, H.D. Um, J.Y. Jung, S.W. Jee, et al., Lossless hybridization between photovoltaic and thermoelectric devices, *Sci Rep* **3**, 2013, 1–6, https://doi.org/10.1038/srep02123.

[80] B. Lorenzi, M. Acciarri and D. Narducci, Suitability of electrical coupling in solar cell thermoelectric hybridization, *Design* **2**, 2018, 32, https://doi.org/10.3390/designs2030032.

[81] G. Li, K. Zhou, Z. Song, X. Zhao and J. Ji, Inconsistent phenomenon of thermoelectric load resistance for photovoltaic–thermoelectric module, *Energy Convers Manag* **161**, 2018, 155–161 https://doi.org/10.1016/j.enconman.2018.01.079.

[82] J. Lin, T. Liao and B. Lin, Performance analysis and load matching of a photovoltaic-thermoelectric hybrid system, *Energy Convers Manag* **105**, 2015, 891–899, https://doi.org/10.1016/j.enconman.2015.08.054.

[83] W. Lin, T.M. Shih, J.C. Zheng, Y. Zhang and J. Chen, Coupling of temperatures and power outputs in hybrid photovoltaic and thermoelectric modules, *Int J Heat Mass Transf* **74**, 2014, 121–127, https://doi.org/10.1016/j.ijheatmasstransfer.2014.02.075.

[84] R. Bjørk and K.K. Nielsen, The performance of a combined solar photovoltaic (PV) and thermoelectric generator (TEG) system, *Sol Energy* **120**, 2015, 187–194, https://doi.org/10.1016/j.solener.2015.07.035.

[85] M. Hajji, H. Labrim, M. Benaissa, A. Laazizi, H. Ez-Zahraouy, E. Ntsoenzok, et al., Photovoltaic and thermoelectric indirect coupling for maximum solar energy exploitation, *Energy Convers Manag* **136**, 2017, 184–191, https://doi.org/10.1016/j.enconman.2016.12.088.

[86] D. Kraemer, K. McEnaney, M. Chiesa and G. Chen, Modeling and optimization of solar thermoelectric generators for terrestrial applications, *Sol Energy* **86**, 2012, 1338–1350, https://doi.org/10.1016/j.solener.2012.01.025.

[87] W.H. Chen, C.C. Wang, C.I. Hung, C.C. Yang and R.C. Juang, Modeling and simulation for the design of thermal-concentrated solar thermoelectric generator, *Energy* **64**, 2014, 287–297, https://doi.org/10.1016/j.energy.2013.10.073.

[88] Z. Liu, S. Zhu, Y. Ge, F. Shan, L. Zeng and W. Liu, Geometry optimization of two-stage thermoelectric generators using simplified conjugate-gradient method, *Appl Energy* **190**, 2017, 540–552, https://doi.org/10.1016/j.apenergy.2017.01.002.

[89] A.S. Al-Merbati, B.S. Yilbas and A.Z. Sahin, Thermodynamics and thermal stress analysis of thermoelectric power generator: influence of pin geometry on device performance, *Appl Therm Eng* **50**, 2013, 683–692, https://doi.org/10.1016/j.applthermaleng.2012.07.021.

[90] H. Hashim, J.J. Bomphrey and G. Min, Model for geometry optimisation of thermoelectric devices in a hybrid PV/TE system, *Renew Energy* **87**, 2016, 458–463, https://doi.org/10.1016/j.renene.2015.10.029.

[91] S. Shittu, G. Li, X. Zhao and X. Ma, Series of detail comparison and optimization of thermoelectric element geometry considering the PV effect, *Renew Energy* **130**, 2019, 930–942, https://doi.org/10.1016/j.renene.2018.07.002.

[92] D.N. Kossyvakis, G.D. Voutsinas and E.V. Hristoforou, Experimental analysis and performance evaluation of a tandem photovoltaic-thermoelectric hybrid system, *Energy Convers Manag* **117**, 2016, 490–500, https://doi.org/10.1016/j.enconman.2016.03.023.

[93] G. Li, X. Zhao, Y. Jin, X. Chen, J. Ji and S. Shittu, Performance analysis and discussion on the thermoelectric element footprint for PV–TE maximum power generation, *J Electron Mater* **47**, 2018, 5344–5351, https://doi.org/10.1007/s11664-018-6421-4

[94] G. Li, X. Chen and Y. Jin, Analysis of the primary constraint conditions of an efficient photovoltaic-thermoelectric hybrid system, *Energies* **10**, 2017, 1–12, https://doi.org/10.3390/en10010020.

[95] Y. Li, S. Witharana, H. Cao, M. Lasfargues, Y. Huang and Y. Ding, Wide spectrum solar energy harvesting through an integrated photovoltaic and thermoelectric system, *Particuology* **15**, 2014, 39–44, https://doi.org/10.1016/j.partic.2013.08.003.

[96] T. Cui, Y. Xuan and Q. Li, Design of a novel concentrating photovoltaic-thermoelectric system incorporated with phase change materials, *Energy Convers Manag* **112**, 2016, 49–60, https://doi.org/10.1016/j.enconman.2016.01.008.

[97] T. Cui, Y. Xuan, E. Yin, Q. Li and D. Li, Experimental investigation on potential of a concentrated photovoltaic-thermoelectric system with phase change materials, *Energy* **122**, 2017, 94–102, https://doi.org/10.1016/j.energy.2017.01.087.

[98] F. Willars-Rodríguez, E. Chavez-Urbiola, P. Vorobiev and Y.V. Vorobiev, Investigation of solar hybrid system with concentrating Fresnel lens, photovoltaic and thermoelectric generators, *Int J Energy Res* **41**, 2017, 377–388, https://doi.org/10.1002/er.361

[99] E. Yin, Q. Li and Y. Xuan, Thermal resistance analysis and optimization of photovoltaic-thermoelectric hybrid system, *Energy Convers Manag* **143**, 2017, 188–202, https://doi.org/10.1016/j.enconman.2017.04.004.

[100] J. Zhang and Y. Xuan, Investigation on the effect of thermal resistances on a highly concentrated photovoltaic-thermoelectric hybrid system, *Energy Convers Manag* **129**, 2016, 1–10, https://doi.org/10.1016/j.enconman.2016.10.006.

[101] W. Pang, Y. Liu, S. Shao and X. Gao, Empirical study on thermal performance through separating impacts from a hybrid PV/TE system design integrating heat sink, *Int Commun Heat Mass Transf* **60**, 2015, 9–12, https://doi.org/10.1016/j.icheatmasstransfer.2014.11.004.

[102] Y.Y. Wu, S.Y. Wu and L. Xiao, Performance analysis of photovoltaic-thermoelectric hybrid system with and without glass cover, *Energy Convers Manag* **93**, 2015, 151–159, https://doi.org/10.1016/j.enconman.2015.01.013.

[103] S. Soltani, A. Kasaeian, H. Sarrafha and D. Wen, An experimental investigation of a hybrid photovoltaic/thermoelectric system with nanofluid application, *Sol Energy* **155**, 2017, 1033–1043, https://doi.org/10.1016/j.solener.2017.06.069.

[104] X.Z. Guo, Y.D. Zhang, D. Qin, Y.H. Luo, D.M. Li, Y.T. Pang, et al., Hybrid tandem solar cell for concurrently converting light and heat energy with utilization of full solar spectrum, *J Power Sources* **195**, 2010, 7684–7690,

https://doi.org/10.1016/j.jpowsour.2010.05.033.

[105] N. Wang, L. Han, H. He, N.-H. Park and K. Koumoto, A novel high-performance photovoltaic–thermoelectric hybrid device, *Energy Environ Sci* **4**, 2011, 3676, https://doi.org/10.1039/c1ee01646f.

[106] Y. Dou, F. Wu, L. Fang, G. Liu, C. Mao, K. Wan, et al., Enhanced performance of dye-sensitized solar cell using Bi2Te3nanotube/ZnO nanoparticle composite photoanode by the synergistic effect of photovoltaic and thermoelectric conversion, *J Powe Sources* **307**, 2016, 181–189, https://doi.org/10.1016/j.jpowsour.2015.12.113.

[107] P. Rai, S. Oh, M. Ramasamy and V.K. Varadan, Photonic nanometer scale metamaterials and nanoporous thermoelectric materials for enhancement of hybrid photovoltaic thermoelectric devices, *Microelectron Eng* **148**, 2015, 104–109, https://doi.org/10.1016/j.mee.2015.09.017.

[108] S. Oh, P. Rai, M. Ramasamy and V.K. Varadan, Fishnet metastructure for IR band trapping for enhancement of photovoltaic-thermoelectric hybrid systems, *Microelectron Eng* **148**, 2015, 117–121, https://doi.org/10.1016/j.mee.2015.10.016.

[109] Y. Xu, Y. Xuan and L. Yang, Full-spectrum photon management of solar cell structures for photovoltaic-thermoelectric hybrid systems, *Energy Convers Manag* **103**, 2015, 533–541, https://doi.org/10.1016/j.enconman.2015.07.007.

[110] Y. Zhang and Y. Xuan, Biomimetic omnidirectional broadband structured surface for photon management in photovoltaic-thermoelectric hybrid systems, *Sol Energy Mater Sol Cells* **144**, 2016, 68–77, https://doi.org/10.1016/j.solmat.2015.08.035.

[111] J. Zhang, Y. Xuan and L. Yang, A novel choice for the photovoltaic-thermoelectric hybrid system: the perovskite solar cell, *Int J Energy Res* **40**, 2016, 1400–1409, https://doi.org/10.1002/er.3532.

[112] L. Xu, Y. Xiong, A. Mei, Y. Hu, Y. Rong, Y. Zhou, et al., Efficient perovskite photovoltaic-thermoelectric hybrid device, *Adv Energy Mater* **8**, 2018, 1–5, https://doi.org/10.1002/aenm.201702937.

[113] R. Rabari, S. Mahmud and A. Dutta, Analysis of combined solar photovoltaic-nanostructured thermoelectric generator system, *Int J Green Energy* **13**, 2016, 1175–1184, https://doi.org/10.1080/15435075.2016.1173040.

[114] B.S. Dallan, J. Schumann and F.J. Lesage, Performance evaluation of a photoelectric-thermoelectric cogeneration hybrid system, *Sol Energy* **118**, 2015, 276–285, https://doi.org/10.1016/j.solener.2015.05.034.

[115] X. Zhang, K. Chau and C. Chan, Design and implementation of a thermoelectric- photovoltaic hybrid energy source for hybrid electric vehicles, *World Electr Veh J* **3**, 2009, 271–281.

[116] X. Zhang and K.T. Chau, An automotive thermoelectric-photovoltaic hybrid energy system using maximum power point tracking, *Energy Convers Manag* **52**, 2011, 641–647, https://doi.org/10.1016/j.enconman.2010.07.041.

[117] K. Fathima, T.M. Saranya, D. Joseph and A. Kumar, A novel method of utilizing hybrid generator as renewable source, *Int J Eng Technol* **7**, 2016, 1972–1976.

[118] D. Jung, K. Kim and S. Jung, Thermal and solar energy harvesting boost converter with time-multiplexing MPPT algorithm, *IEICE Electron Express* **13**, 2016, 1–9, https://doi.org/10.1109/TEC.2006.874230.

[119] V. Verma, A. Kane and B. Singh, Complementary performance enhancement of PV energy system through thermoelectric generation, *Renew Sustain Energy Rev* **58**, 2016, 1017–1026, https://doi.org/10.1016/j.rser.2015.12.212.

[120] T.H. Kwan and X. Wu, The Lock-On Mechanism MPPT algorithm as applied to the hybrid photovoltaic cell and thermoelectric generator system, *Appl Energy* **204**, 2017, 873–886, https://doi.org/10.1016/j.apenergy.2017.03.036.

[121] H. Yu, Y. Li, Y. Shang and B. Su, Design and investigation of photovoltaic and thermoelectric hybrid power source for wireless sensor networks, *3rd IEEE Int Conf Nano/Micro Eng Mol Syst NEMS* 2008, 196–201, https://doi.org/10.1109/NEMS.2008.4484317.

[122] V. Leonov, T. Torfs, R.J.M. Vullers and C. Van Hoof, Hybrid thermoelectric-photovoltaic generators in wireless electroencephalography diadem and electrocardiography shirt, *J Electron Mater* **39**, 2010, 1674–1680, https://doi.org/10.1007/s11664-010-1230-4.

[123] Y. Da, Y. Xuan and Q. Li, From light trapping to solar energy utilization: a novel photovoltaic-thermoelectric hybrid system to fully utilize solar spectrum, *Energy* **95**, 2016, 200–210, https://doi.org/10.1016/j.energy.2015.12.024.

[124] T.H. Kwan and X. Wu, Power and mass optimization of the hybrid solar panel and thermoelectric generators, *Appl Energy* **165**, 2016, 297–307, https://doi.org/10.1016/j.apenergy.2015.12.016.

[125] A. Rezania, D. Sera and L.A. Rosendahl, Coupled thermal model of photovoltaic-thermoelectric hybrid panel for sample cities in Europe, *Renew Energy* **99**, 2016, 127–135, https://doi.org/10.1016/j.renene.2016.06.045.

[126] M.R. Ariffin, S. Shafie, W. Hassan, N. Azis and M.E. Ya'acob, Conceptual design of hybrid photovoltaic- thermoelectric generator (PV/TEG) for automated greenhouse system, In: *2017 IEEE 15th student conf. Res. Dev.,* 2017, 309–314.

[127] A. Makki, S. Omer, Y. Su and H. Sabir, Numerical investigation of heat pipe-based photovoltaic-thermoelectric generator (HP-PV/TEG) hybrid system, *Energy Convers Manag* **112**, 2016, 274–287, https://doi.org/10.1016/j.enconman.2015.12.069.

[128] G. Li, X. Zhao and J. Ji, Conceptual development of a novel photovoltaic-thermoelectric system and preliminary economic analysis, *Energy Convers Manag* **126**, 2016, 935–943 https://doi.org/10.1016/j.enconman.2016.08.074.

[129] P. Huen and W.A. Daoud, Advances in hybrid solar photovoltaic and thermoelectric generators, *Renew Sustain Energy Rev* **72**, 2017, 1295–1302, https://doi.org/10.1016/j.rser.2016.10.042.

[130] D.L. Chubb and B.S. Good, A combined thermophotovoltaic-thermoelectric energy converter, *Sol Energy* **159**, 2018, 760–767, https://doi.org/10.1016/j.solener.2017.11.030.

[131] K. Teffah and Y. Zhang, Modeling and experimental research of hybrid PV-thermoelectric system for high concentrated solar energy conversion, *Sol Energy* **157**, 2017, 10–19, https://doi.org/10.1016/j.solener.2017.08.017.

[132] K. Teffah, Y. Zhang and X. Mou, Modeling and experimentation of new thermoelectric cooler–thermoelectric generator module, *Energies* **11**, 2018, 576, https://doi.org/10.3390/en11030576.

[133] K. Yoshikawa, H. Kawasaki, W. Yoshida, T. Irie, K. Konishi, K. Nakano, et al., Silicon heterojunction solar cell with interdigitated back contacts for a photoconversion efficiency over 26%, *Nat Energy* **2**, 2017, 17032.

[134] J. Benick, A. Richter, R. Müller, H. Hauser, F. Feldmann, P. Krenckel, et al., High-efficiency n-type HP mc silicon solar cells, *IEEE J Photovoltaics* **7**, 2017, 1171–1175, https://doi.org/10.1109/JPHOTOV.2017.2714139.

[135] B.M. Kayes, H. Nie, R. Twist, S.G. Spruytte, F. Reinhardt, I.C. Kizilyalli, et al., 27.6% Conversion efficiency, a new record for single-junction solar cells under 1 sun illumination, *Conf Rec IEEE Photovolt Spec Conf* 2011, 000004–000008, https://doi.org/10.1109/PVSC.2011.6185831.

[136] M. Wanlass, Systems and methods for advanced ultra-high-performance, *InP solar cells* **9** (590), 2017, 131 B2.

[137] Solar Frontier Press Release, Solar frontier achieves world record thin-film solar cell efficiency of 22.9%, 20 December 2017 http://www.solar-frontier.com/eng/news/2017/1220_press.html, Accessed 10 November 2018.

[138] J.-L. Wu, Y. Hirai, T. Kato, H. Sugimoto and V. Bermudez, New world record efficiency up to 22.9% for Cu(in,Ga)(Se,S)2 thin-film solar cells, 2018.

[139] First Solar Press Release, First Solar builds the highest efficiency thin film PV cell on record, 5 August 2014 http://investor.firstsolar.com/news-releases/news-release-details/first-solar-builds-highest-efficiency-thin-film-pv-cell-record, Accessed 10 November 2018.

[140] T. Matsui, A. Bidiville, K. Maejima, H. Sai, T. Koida, T. Suezaki, et al., High-efficiency amorphous silicon solar cells: impact of deposition rate on metastability, *Appl Phys Lett* **106**, 2015, , 053901https://doi.org/10.1063/1.4907001.

[141] W.S. Yang, J.H. Noh, N.J. Jeon, Y.C. Kim, S. Ryu, J. Seo, et al., High-performance photovoltaic perovskite layers fabricated through intramolecular exchange, *Science* **348** (80-), 2015, 1234–1237, doi:10/f7fzcf.

[142] R. Komiya, A. Fukui, N. Murofushi, N. Koide, R. Yamanaka and H. Katayama, Improvement of the conversion efficiency of a monolithic type dye- sensitized solar cell module, In: *Tech. Dig. 21st int. Photovolt. Sci. Eng. Conf., Fukuoka,* 2011.

[143] S. Mori, H. Oh-oka, H. Nakao, T. Gotanda, Y. Nakano, H. Jung, et al., Organic photovoltaic module development with inverted device structure, *MRS Proc* **1737**, 2015, https://doi.org/10.1557/opl.2015.540, mrsf14-1737-u17-02.

[144] M. Mizoshiri, M. Mikami and K. Ozaki, Thermal-photovoltaic hybrid solar generator using thin-film thermoelectric modules, *Jpn J Appl Phys* **51**, 2012, 2–7, https://doi.org/10.1143/JJAP.51.06FL07.

[145] E. Elsarrag, H. Pernau, J. Heuer, N. Roshan, Y. Alhorr and K. Bartholomé, Spectrum splitting for efficient utilization of solar radiation: a novel photovoltaic–thermoelectric power generation system, *Renewables Wind Water, Sol* **2**, 2015, 16, https://doi.org/10.1186/s40807-015-0016-y.

[146] E.J.H. Skjølstrup and T. Søndergaard, Design and optimization of spectral beamsplitter for hybrid thermoelectric-photovoltaic concentrated solar energy devices, *Sol Energy* **139**, 2016, 149–156, https://doi.org/10.1016/j.solener.2016.09.036.

[147] K.P. Sibin, N. Selvakumar, A. Kumar, A. Dey, N. Sridhara, H.D. Shashikala, et al., Design and development of ITO/Ag/ITO spectral beam splitter coating for photovoltaic-thermoelectric hybrid systems, *Sol Energy* **141**, 2017, 118–126, https://doi.org/10.1016/j.solener.2016.11.027.

[148] Mustofa, Z. Djafar, Syafaruddin and W.H. Piarah, A new hybrid of photovoltaic-thermoelectric generator with hot mirror as spectrum splitter, *J Phys Sci* **29**, 2018, 63–75, https://doi.org/10.21315/jps2018.29.s2.6.

[149] C. Shou, Z. Luo, T. Wang, W. Shen, G. Rosengarten, W. Wei, et al., Investigation of a broadband TiO2/SiO2optical thin-film filter for hybrid solar power systems, *Appl Energy* **92**, 2012, 298–306, https://doi.org/10.1016/j.apenergy.2011.09.028.

[150] M.M.M. Daud, N.B.M. Nor and T. Ibrahim, Novel hybrid photovoltaic and thermoelectric panel, In: *2012 IEEE int power eng optim conf PEOCO 2012 - conf proc,* 2012, 269–274, https://doi.org/10.1109/PEOCO.2012.6230873.

[151] Y. Zhang, J. Fang, C. He, H. Yan, Z. Wei and Y. Li, Integrated energy-harvesting system by combining the advantages of polymer solar cells and thermoelectric devices, *J Phys Chem C* **117**, 2013, 24685–24691, https://doi.org/10.1021/jp4044573.

[152] J. Zhang, Y. Xuan and L. Yang, Performance estimation of photovoltaic-thermoelectric hybrid systems, *Energy* **78**, 2014, 895–903, https://doi.org/10.1016/j.energy.2014.10.087.

[153] T. Liao, B. Lin and Z. Yang, Performance characteristics of a low concentrated photovoltaic- thermoelectric hybrid power generation device, *Int J Therm Sci* **77**, 2014, 158–164, https://doi.org/10.1016/j.ijthermalsci.2013.10.013.

[154] H. Chen, N. Wang and H. He, Equivalent circuit analysis of photovoltaic – thermoelectric hybrid device with different TE module structure, *Adv Condens Matter Phys* 2014, 1–16, https://doi.org/10.1155/2014/824038.

[155] O. Beeri, O. Rotem, E. Hazan, E.A. Katz, A. Braun and Y. Gelbstein, Hybrid photovoltaic-thermoelectric system for concentrated solar energy conversion: experimental realization and modeling, *J Appl Phys* **118**, 2015, , 115104https://doi.org/10.1063/1.4931428.

[156] F. Attivissimo, A. Di Nisio, A.M.L. Lanzolla and M. Paul, Feasibility of a photovoltaic-thermoelectric generator: performance analysis and simulation results, *IEEE Trans Instrum Meas* **64**, 2015, 1158–1169, https://doi.org/10.1109/TIM.2015.2410353.

[157] B. Luo, Y. Deng, Y. Wang, M. Gao, W. Zhu, H.T. Hashim, et al., Synergistic photovoltaic-thermoelectric effect in a nanostructured CdTe/Bi2Te3 heterojunction for hybrid energy harvesting, *RSC Adv* **6**, 2016, 114046–114051, https://doi.org/10.1039/C6RA20149K.

[158] W. Pang, H. Yu, Y. Zhang and H. Yan, Electrical characteristics of a hybrid photovoltaic/thermoelectric generator system, *Energy Technol* **6**, 2017, 1248–1254, https://doi.org/10.1002/ente.201700801.

[159] D.T. Cotfas, P.A. Cotfas, O.M. Machidon and D. Ciobanu, Investigation of the photovoltaic cell/thermoelectric element hybrid system performance, *IOP Conf Ser Mater Sci Eng* **133**, 2016, 1–10, https://doi.org/10.1088/1757-899X/133/1/012037.

[160] Z. Zhou, J. Yang, Q. Jiang, W. Li, Y. Luo, Y. Hou, et al., Large improvement of device performance by a synergistic effect of photovoltaics and thermoelectrics, *Nano Energy* **22**, 2016, 120–128, https://doi.org/10.1016/j.nanoen.2016.02.018.

[161] T.H. Kil, S. Kim, D.H. Jeong, D.M. Geum, S. Lee, S.J. Jung, et al., A highly-efficient, concentrating-photovoltaic/thermoelectric hybrid generator, *Nano Energy* **37**, 2017, 242–247, https://doi.org/10.1016/j.nanoen.2017.05.023.

[162] D. Li, Y. Xuan, Q. Li and H. Hong, Exergy and energy analysis of photovoltaic-thermoelectric hybrid systems, *Energy* **126**, 2017, 343–351, https://doi.org/10.1016/j.energy.2017.03.042.

[163] Z. Liu, B. Sun, Y. Zhong, X. Liu, J. Han, T. Shi, et al., Novel integration of carbon counter electrode based perovskite solar cell with thermoelectric generator for efficient solar energy conversion, *Nano Energy* **38**, 2017, 457–466, https://doi.org/10.1016/j.nanoen.2017.06.016.

[164] Y. Zhang and Y. Xuan, Preparation of structured surfaces for full-spectrum photon management in photovoltaic-thermoelectric systems, *Sol Energy Mater Sol Cells* **169**, 2017, 47–55, https://doi.org/10.1016/j.solmat.2017.04.036.

[165] H. Machrafi, Enhancement of a photovoltaic cell performance by a coupled cooled nanocomposite thermoelectric hybrid system, using extended thermodynamics, *Curr Appl Phys* **17**, 2017, 890–911, https://doi.org/10.1016/j.cap.2017.03.001.

[166] Y. Jeyashree, P.B. Hepsiba, S. Indirani, A.D. Savio and Y. Sukhi, Solar energy harvesting using hybrid photovoltaic and thermoelectric generating system, *Glob J Pure Appl Math* **13**, 2017, 5935–5944.

[167] Y. Nishijima, R. Komatsu, T. Yamamura, G. Seniutinas and J. Saulius, Design concept of a hybrid photo-voltaic/thermal conversion cell for mid-infrared light energy harvester, *Opt Mater Express* **7**, 2017, 3484–3493, https://doi.org/10.4161/19336918.2014.994893.

[168] D. Li, Y. Xuan, E. Yin and Q. Li, Conversion efficiency gain for concentrated triple-junction solar cell system through thermal management, *Renew Energy* **126**, 2018, 960–968, https://doi.org/10.1016/j.renene.2018.04.027.

Highlights

- A detailed review of photovoltaic thermal management is presented.
- The role of thermoelectric generator in hybrid photovoltaic enhancement is explained.
- Research focus areas in hybrid photovoltaic/thermoelectric generator are discussed.
- Recommendations for future research on hybrid PV/TEG are presented.

Queries and Answers

Query: Please confirm that the provided emails “Guiqiang.Li@hull.ac.uk, Xudong.Zhao@hull.ac.uk” are the correct address for official communication, else provide an alternate e-mail address to replace the existing one, because private e-mail addresses should not be used in articles as the address for communication.

Answer: Yes, the provided emails are correct for official communication.

Query: Please note that ’Fig.23, Fig.24’ was/were not cited in the text. Please check that the citation(s) suggested by the copyeditor are in the appropriate place, and correct if necessary.
Answer: No, the citations suggested are not in the appropriate place. An instruction on their right location has been given.

Query: Have we correctly interpreted the following funding source(s) and country names you cited in your article: Innovate UK, United Kingdom; EPSRC, United Kingdom?
Answer: Yes

Query: Please confirm that given names and surnames have been identified correctly and are presented in the desired order and please carefully verify the spelling of all authors’ names.
Answer: Yes

Query: Your article is registered as a regular item and is being processed for inclusion in a regular issue of the journal. If this is NOT correct and your article belongs to a Special Issue/Collection please contact l.daniel@elsevier.com immediately prior to returning your corrections.
Answer: Yes this is correct.